THE NF-κB SIGNAL TRANSDUCTION PATHWAY IN AORTIC ENDOTHELIAL CELLS IS PRIMED FOR ACTIVATION IN REGIONS PREDISPOSED TO ATHEROSCLEROTIC LESION FORMATION

by

Leena Hajra

A thesis submitted in conformity with the requirements
for the degree of Master of Science
Graduate Department of Laboratory Medicine and Pathobiology
University of Toronto

ABSTRACT

The NF-κB signal transduction pathway in aortic endothelial cells is primed for activation in regions predisposed to atherosclerotic lesion formation, Master of Science 2000, Leena Hajra, Department of Laboratory Medicine and Pathobiology, University of Toronto

Atherosclerotic lesions form at distinct sites in the arterial tree, suggesting that hemodynamic forces influence the initiation of atherogenesis. Several systemic risk factors for atherogenesis have been shown to activate NF-κB and NF-κB regulates multiple genes important in lesion initiation. If NF-κB plays a role in atherogenesis, then the activation of this signal transduction pathway in arterial endothelium should show topographic variation. The expression of NF-κB/IκB components and NF-κB activation were evaluated by specific antibody staining, *en face* confocal microscopy and image analysis of endothelium in regions of mouse proximal aorta with high and low probability (HP and LP) for atherosclerotic lesion development. HP region endothelial cells visualized by silver nitrate staining had a polygonal shape in contrast to LP region cells that were uniformly elongated parallel to the direction of blood flow. In control C57BL/6 mice, expression levels of p65, IκBα and IκBβ were 5 to 18 fold higher in the HP region, yet NF-κB was activated in a minority of endothelial cells. This suggested that NF-κB signal transduction was primed for activation in HP regions upon encountering an activation stimulus. LPS treatment or feeding LDL receptor knockout mice an atherogenic diet resulted in NF-κB activation and upregulated expression of NF-κB-inducible genes predominantly in HP region endothelium. Preferential regional activation of endothelial NF-κB by systemic stimuli, including hypercholesterolemia, may contribute to the localization of atherosclerotic lesions at sites with high steady-state expression levels of NF-κB/IκB components.

THESIS OUTLINE

ABSTRACT

ACKNOWLEDGEMENTS

ABBREVIATIONS

CHAPTER 1 - Overview

ATHEROSCLEROSIS - AN INTRODUCTION
LESION INITIATION
ENDOTHELIAL CELL DYSFUNCTION
PREDILECTION SITES FOR LESION FORMATION
NF-κB SIGNAL TRANSDUCTION - AN INTRODUCTION
NF-κB AND ATHEROGENESIS
NF-κB AND HEMODYNAMICS

RATIONALE AND HYPOTHESIS

CHAPTER 2 - Development of a mouse model to examine gene expression in regions with high and low probability for atherosclerotic lesion formation

OBJECTIVES

MATERIALS AND METHODS

RESULTS

CHAPTER 3 - Immunofluorescent examination of NF-κB signal transduction components in HP vs. LP regions.

OBJECTIVES

MATERIALS AND METHODS

RESULTS

CHAPTER 4 - Discussion and Future Directions

DISCUSSION
SUMMARY
FUTURE DIRECTIONS
REFERENCES

ACKNOWLEDGMENTS

I would like to acknowledge my supervisor Dr. Myron Cybulsky for his steady guidance and support over the last two years. Secondly, I want to say thanks to my mother for her encouragement and to my father for initiating my interest in science. Thank-you to Laila and Leepy for all their support, especially Leepy for helping with all this typing.

ABBREVIATIONS

ApoE - Apolipoprotein E

Egr-1 - Early growth response - 1

FGF - fibroblast growth factor

GM-CSF - granulocyte macrophage colony stimulating factor

HP - high probability

HUVEC - human umbilical vein endothelial cell

IκB - inhibitors of nuclear factor kappa B

ICAM-1 - intercellular adhesion molecule - 1

ICAM-2 - intercellular adhesion molecule - 2

IKK - IκB kinase

IL-1 - interleukin - 1

LDLR $^{-/-}$ - low density lipoprotein receptor knockout

LP - low probability

LPS - lipopolysaccharide

MCP-1 - monocyte chemoattractant protein - 1

M-CSF- macrophage colony stimulating factor

NF-κB - nuclear factor kappa B

ORO - oil red O

OxLDL - oxidized low density lipoprotein

PBS - phosphate buffered saline

PDGF - platelet derived growth factor

PECAM-1 - platelet endothelial cell adhesion molecule - 1

TGF - transforming growth factor

TNF-α - tumour necrosis factor - α

VCAM-1 - vascular cell adhesion molecule - 1

CHAPTER ONE

ATHEROSCLEROSIS – AN INTRODUCTION

At one time, atherosclerosis was thought to be a degenerative disease that was an inevitable consequence of aging. Research in the last two decades has shown that atherosclerosis is neither a degenerative disease nor inevitable. In fact, the lesions of atherosclerosis represent a series of highly specific cellular and molecular responses that can best be described, in combination, as a chronic inflammatory process.

A disease of large elastic and muscular arteries, atherosclerosis is the principle cause of heart attack, stroke and gangrene of the extremities and is responsible for approximately 50% of all mortality in the USA, Europe and Japan (1). It is potentiated by systemic risk factors, including lipoprotein disorders, diabetes mellitus, smoking and hypertension, although to date, they have not been linked to a common pathogenic mechanism (2).

As proposed by Russell Ross, atherosclerosis may best be described as a "defense mechanism gone awry." (3) This hypothesis suggests that atherosclerotic lesions represent a protective response to various forms of insult to the artery wall. Depending upon the nature and duration of the insult, this protective response may become excessive and in its excess become a disease process.

Initially, different forms of insult to the endothelium and to the cells of the artery wall begin at specific sites in the arterial tree with a chronic inflammatory response featuring peripheral blood monocytes and T lymphocytes, which adhere to the endothelium and invade the artery wall (4). At these sites monocytes are converted to macrophages. Macrophages engulf oxidized low density lipoprotein (LDL) particles, become activated and express various cytokines and growth factors (3, 5). These genes in turn cause macrophage replication as well as smooth muscle cell migration and proliferation within the intima of the artery (Figure 1). Collectively,

FIGURE 1 - Structure of the artery wall. The layers of the artery wall are illustrated starting with the innermost endothelial cell monolayer and ending with the outermost adventitial layer.

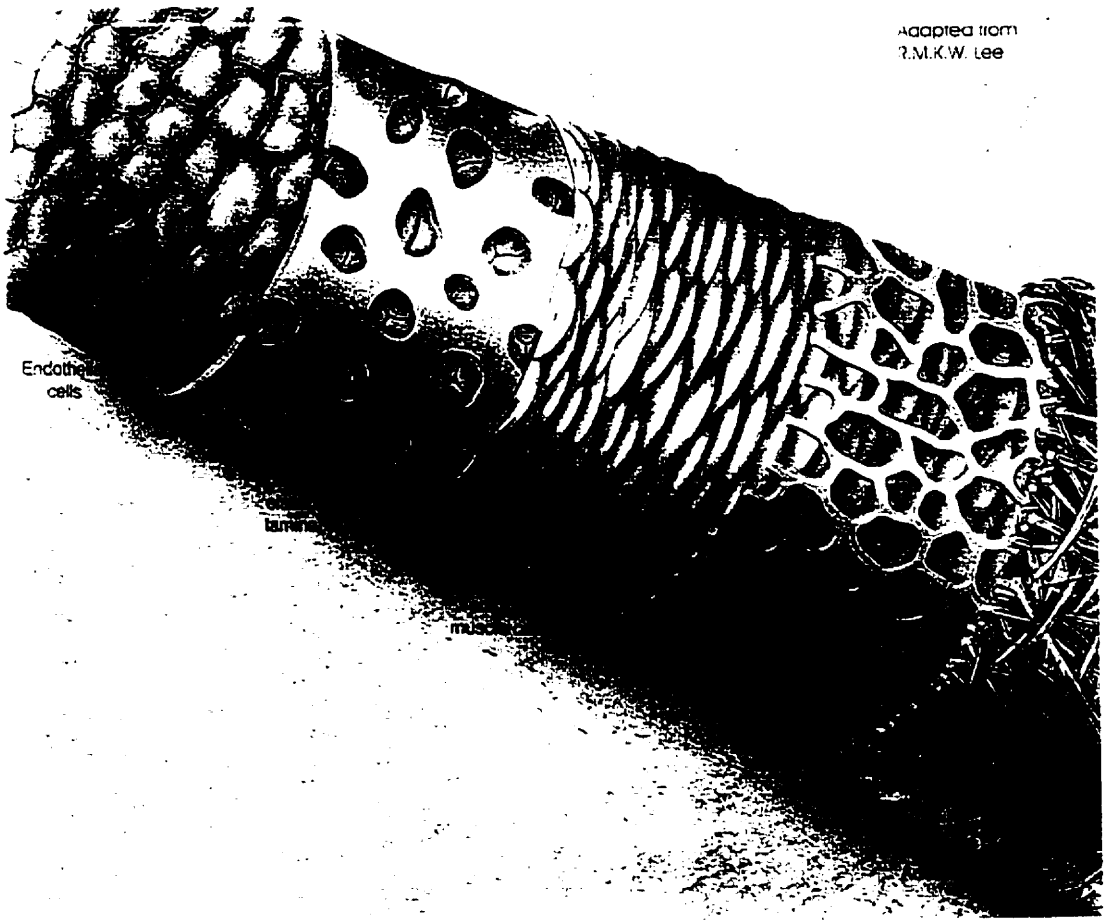
Adapted from
P.M.K.W. Lee
Endothe
cells

these cells form the early fatty streak lesion in atherosclerosis composed primarily of lipid engorged macrophages, called foam cells. The lesions of atherosclerosis differ from other lesions in the arterial tree by their localization largely within the intima. The intermediate lesion represents a stage during which replication of both macrophages and smooth muscle cells occurs, resulting in alternating layers of macrophages, T cells and smooth muscle that form varying amounts of connective tissue. A fibrous cap forms over the lesion, which is possibly an attempt to protect the artery wall by providing some tensile strength to the weakened site. With continued cell replication, necrosis, lipid accumulation and connnective tissue formation, the lesions increase in size forming fibrous plaques. These fibrous plaques or advanced lesions may project into the lumen and impede blood flow. They are covered by a dense cap of connective tissue with embedded smooth muscle cells that overlays a core of lipid and necrotic debris (3, 5). Ultimately, plaque rupture results in hemorrhage, thrombosis and occlusion of the artery, leading to clinical consequences.

The development of the fatty streak and progression to intermediate and advanced lesions have been observed in a large number of experimental animals, including rabbits (6, 7), swine (8, 9), pigeons (10), non human primates (11, 12) and most recently in a series of genetically modified transgenic mice (13, 14). The genetically modified mice, in particular, the homozygous apolipoprotein E (Apo-E)-deficient and LDL-receptor-deficient mice, offer unique opportunities to study atherogenesis and intervening approaches in a small murine model that can be genetically modified. Crossbreeding these mice into other relevant backgrounds, offer opportunity to understand the roles of specific molecules in the process of atherogenesis and to develop specific modes of intervention.

LESION INITIATION

The earliest grossly detectable lesion of atherosclerosis is the fatty streak, which consists of an accumulation of lipid within macrophages, or foam cells, in the intima of the artery and appears as a yellow discoloration on the arterial luminal surface . The mechanistic understanding of events leading to lesion initiation is critical, since components of the fatty streak. which itself is not significant are also responsible for latter events leading to significant disease.

Fatty streak development begins with lipoprotein transport into the artery wall. This concentration dependent process does not require receptor mediated endocytosis (15, 16). The fact that atherosclerosis is induced in multiple species by mutations in the LDL receptor suggest elevations in LDL may induce all components of the atherosclerotic reaction. The LDL is rapidly transported across an intact endothelium and becomes trapped in a three dimensional network of fibers in the subendothelial space (17). Here, LDL particles are preferentially retained in the artery wall at sites predisposed to lesion formation (18). The oxidative modification of the trapped LDL is thought to occur in two stages. The first stage occurs before monocytes are recruited and results in the oxidization of lipids in LDL with little change in apoB (the major protein of LDL). The second stage begins when monocytes are recruited to the lesion (as a result of endothelial cell dysfunction), convert into macrophages, and contribute their enormous oxidative capacity. In the second stage, LDL lipids are further oxidized, but the protein portion of LDL is also modified, leading to a loss of recognition by the LDL receptor and a shift to recognition by the scavenger receptors (oxLDL receptor) on macrophages (19). This shift leads to cellular uptake of the LDL by receptors that are not regulated by the cholesterol content of the cell. These cholesterol loaded cells have a foamy cytoplasm and are called foam cells, which are the hallmark of the arterial fatty streak.

ENDOTHELIAL CELL DYSFUNCTION

Prior to foam cell formation, the monocytes must first be recruited to the endothelium. Although the source of injury to the endothelium in propagating this recruitment remains unclear, multiple candidates have been proposed including changes in cytokines (20), viral infection (21), variations in shear stress (22), free radical and oxidized lipids (23, 24) and homocysteine (25). These changes cause the endothelium to become "activated" or dysfunctional, ultimately resulting in monocyte recruitment, transmigration and replication.

Vascular endothelium forms the biologic interface between circulating blood components and all the various tissues of the body and is uniquely situated to monitor systemic and locally generated stimuli and alter its functional state. In normal homeostasis this adaptive process occurs continually(26). However, non-adaptive changes in endothelial structure and function, provoked by pathophysiological stimuli can result in alterations in the interactions of endothelium with components of the circulating blood and vessel wall. These alterations include enhanced permeability to plasma lipoproteins, hyperadhesiveness for blood leukocytes, and functional imbalances in local pro and antithrombotic factors, growth stimulators and inhibitors, and vasoactive substances. These manifestations collectively termed endothelial cell dysfunction, play an important role in all stages of atherogenesis (27, 28).

One of the earliest morphologically detectable cellular events in atherogenesis is the adherence of circulating blood monocytes to the intact endothelium (29). The monocytes initially adhere as a result of expression by the endothelium of a series of molecules termed selectins (E-, and P-selectin) that can cause the monocytes to roll and attach on the surface of the endothelium (30). Endothelial expression of adhesion molecules VCAM-1 and ICAM-1 result in firm adherence and spreading of the monocytes on the endothelial surface (29, 31). Endothelial cells may promote monocyte entry into the artery by formation of specific chemotactic agents such as MCP-1 and oxLDL, which form a concentration gradient, allowing directed migration of monocytes from the luminal surface of the endothelium to the

artery (32-34) . The endothelium also interacts intimately with other lesion constituents such as macrophages, smooth muscle cells and platelets to facilitate lesion formation. Stimulated by various growth factors and cytokines produced by surrounding cells, endothelial cells may in turn express genes for growth regulating molecules and activating factors (PDGF, bFGF, TGF-β, M-CSF, GM-CSF) which further facilitates lesion growth by proliferation and activation of cells.

PREDILECTION SITES FOR LESION FORMATION

The anatomically localized pattern of the earliest lesions of atherosclerosis strongly implicates hemodynamic forces in this disease process (35). In particular, atherosclerotic lesions occur most frequently in association with arterial geometries such as branch points, bifurcations and curvatures (36). By surgically altering vessels, several groups have induced arterial lesions, further supporting the role of hemodynamics in lesion development (37, 38). Detailed fluid mechanical analyses of lesion-susceptible vascular geometries have revealed that these locations are exposed to disturbed laminar shear with spatial and temporal shear stress gradients as opposed to uniform laminar shear (39-41). This shear stress regime is characterized by regions of flow seperation, recirculation and reattachment (42). In addition studies have shown that lesions tend to occur in regions of low shear stress, where there are disturbed flow patterns, backflow and eddy currents (43). Regions with decreased shear may be significant to the disease process since a longer time is available for contact between white blood cells and endothelium. If adhesive molecules form on the surface of the endothelium, there would be greater opportunity for monocytes to adhere, spread and crawl between the endothelium into the vessel wall. Studies have shown preferential upregulation of adhesion molecules VCAM-1 and ICAM-1 in endothelium of atherosclerotic prone regions in normocholesterolemic animals (44, 45). Increased LDL retention (18) and increased monocyte adherence (46) have also been observed in lesion prone sites after short term cholesterol feeding. These events could then set the stage for development of the intial fatty streak at predilection sites for lesion formation.

Several *in vivo* morphometric studies, both in native and surgically altered vessels, have demonstrated that endothelial cell structure is modified in regions of disturbed flow, with cells displaying polygonal, nonoriented shapes, in contrast to the elongation and alignment of endothelial cells in regions of unidirectional flow (47-50). It is believed that the endothelial cells act as signal transducers of shear stress to modulate smooth muscle cell regulation of vasomotor tone in the artery wall. Shear stresses are very small forces that cause minimal

deformation of the media (51) whereas the endothelial cells that are in direct contact with the flowing blood are greatly sensitive to shear. In addition, numerous shear driven changes in the endothelium have been documented including cell shape changes, cell proliferation (52), expression of adhesion molecules (29), production of matrix (53), release of vasoactive substances and growth factors (54, 55). Thus, shear stress may be a critical player in lesion development. In concert with other pathophysiological stimuli, disturbed flow and low shears may activate various signal transduction cascades ultimately leading to endothelial cell dysfunction and lesion initiation. In this way, hemodynamics may explain, the predisposition for lesion formation, in certain arterial regions, in the presence of systemic risk factors that act throughout the arterial tree.

NF-κB – An Introduction

The NF-κB/Rel family of proteins consist of homo or heterodimers (reviewed by Ghosh and Karin (56, 57). Subunits include NF-κB1 (p50), NF-κB2 (p52, p49, p50B), p65 (RelA), RelB and c-Rel. All are expressed ubiquitously except for RelB and c-Rel, which are largely restricted to lymphoid and hematopoietic cells, respectively. In cultured endothelial cells, p50/p65 is the predominant NF-κB species (58). NF-κB subunits share a Rel homology domain, which is a 300 amino acid N-terminal region that mediates several key functions, including dimerization, DNA binding, nuclear translocation and binding of inhibitors. The C-terminal region of most subunits contains a transactivation domain. In quiescent cells, NF-κB is localized in the cytoplasm where it is retained through association with an inhibitor (56, 57). Inhibitors of NF-κB (IκBs) include IκBα, IkBβ, IkBε, bcl-3, p105 (precursor of p50) and p100 (precursor of p52) and IkBχ (a 70 kD protein arising by alternate promoter usage in the p105 gene). IκBs contain 6 or more ankyrin repeats, a N-terminal regulatory domain and a C-terminal domain that contains a PEST motif involved in basal turnover. Different IκBs bind preferentially to different NF-κB dimers and sterically hinder binding of importins to the nuclear localization sequence of NF-κB subunits.

Diverse stimuli can activate NF-κB, through phosphorylation and activation of the IκB kinase complex (56, 57). Activated IκB kinases phosphorylate IκBs leading to their polyubiquitination and degradation by 26S proteasomes. NF-κB dimers are transported to the nucleus where they bind to the major grove of DNA and transactivate gene expression through interactions with other transcription factors and coactivators (Figure 2) (59). Each NF-κB subunit has different DNA binding and transactivation properties. Activation of NF-κB provides negative feedback to this signaling pathway by rapidly upregulating IkBα expression, resulting in replenishment of the cytoplasmic pool of its inhibitor (60-63). IkBα contains a nuclear export sequence and after associating with DNA-bound NF-κB, it binds exportins and transports NF-κB back to the cytoplasm (64, 65).

FIGURE 2 - The NF-κB signal transduction pathway. In resting cells, p65-p50 (the prototypic NF-κB heterodimer), is complexed to an inhibitor IκB, which retains the entire complex in the cytoplasm. Upon encountering appropriate activation stimuli the p65-p50 subunit is phosphorylated by the IKK complex, polyubiquitinated and degraded by the 26S proteosome, thereby allowing p65-p50 to translocate to the nucleus and transactivate the expression of target genes.

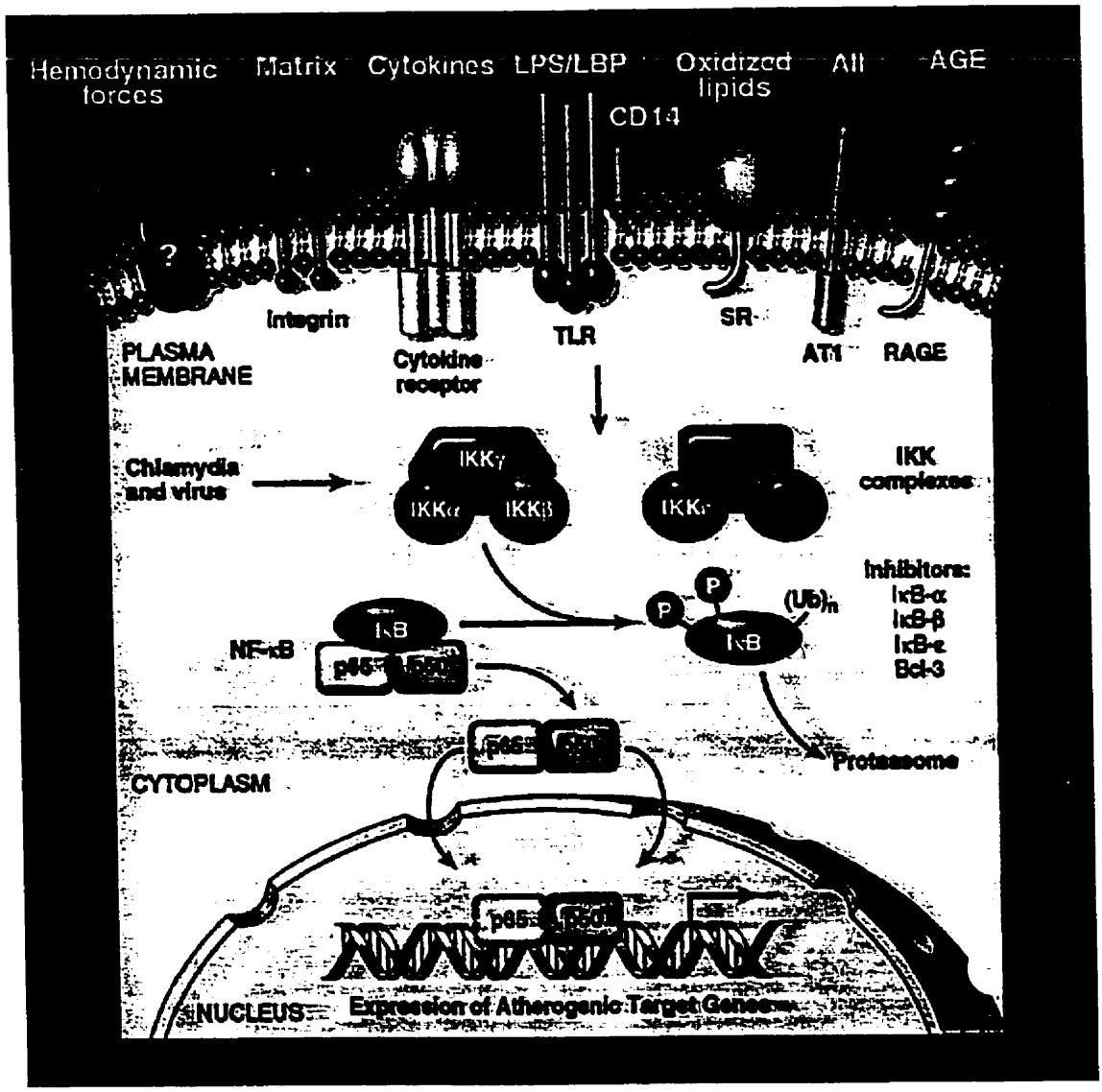
Hemodynamic forces
Matrix
Cytokines
LPS/LBP
Oxidized lipids
AII
AGE
CD14
?
Integrin
PLASMA MEMBRANE
Cytokine receptor
TLR
SR
AT1
RAGE
Chlamydia and virus
IKKγ
IKKα
IKKβ
IKKγ
IKK complexes
Inhibitors:
IκB-α
IκB-β
IκB-ε
Bcl-3
P
P
(Ub)n
IκB
IκB
NF-κB
p65
p50
p65
p50
Proteasome
CYTOPLASM
p65
p50
NUCLEUS
Expression of Atherogenic Target Genes

NF-κB and Atherogenesis

NF-κB may be activated by a variety of stimuli, many of which have been strongly linked to the progression of atherosclerotic disease. For example, oxidized lipoproteins activate NF-κB in HUVEC's and THP-1 monocytes and this effect can be attenuated by treatment with the antioxidant lacidipine or the proteosome inhibitor PSI (66, 67). Cytokines such as TNF-α and IL-1 which are important in the induction of adhesion molecules can also activate NF-κB in HUVECs (68). Endothelial cells infected with Chlamydia pneumoniae, a virus recently demonstrated to be present in atherosclerotic lesions, showed increased NF-κB nuclear translocation as compared to uninfected controls (69).

Many genes whose products are involved in the atherosclerotic process are regulated by NF-κB including the adhesion molecules VCAM-1, ICAM-1 and E-selectin (70, 71) , the chemoattractant MCP-1 (72, 73) and growth factors such as PDGF (74).

Studies have shown correlations between NF-κB activation and expression of κB – target genes important in early lesion development. In HUVEC's, increased NF-κB activation correlated with increased expression of VCAM-1, ICAM-1 and E-selectin after TNF-α stimulation (71). In a rabbit model of atherosclerosis, increased arterial expression of MCP-1 and PDGF in the intima and media correlated with increased NF-κB activation in macrophages and smooth muscles cells (74). Recently, increased NF-κB activation has been shown in advanced human atherosclerotic plaques (75).

Taken together, these studies suggest a potentially critical role for NF-κB signal transduction in atherogenesis since; multiple activators of NF-κB also induce lesions, many genes important in lesion initiation are regulated by NF-κB and various cell types within lesions including endothelial cells, smooth muscle cells and macrophages show increased NF-κB activation in response to atherogenic stimuli. In this regard, NF-κB may exaggerate the atherosclerotic process through coordinated activation of several inflammatory genes.

NF-κB and Hemodynamics

It is important to highlight the effect of shear stress on NF-κB signal transduction, since hemodynamics influence the localization of lesions. Initial studies showed increased NF-κB activation in response to low shear stress as compared to high shear stress in cultured endothelial cells, using a parallel plate flow chamber (76). Subsequent studies went on to show that pulsatile, and or disturbed flow increased NF-κB activation as compared to laminar flow (77, 78). Finally, low shear applied to human aortic endothelial cells induced NF-κB activation, VCAM-1 expression and monocyte adhesion and these effects were blocked by treatment with an antioxidant (79).

Since lesion-prone regions tend to correlate with regions of low shear and disturbed flow patterns, the above evidence indicates that effects of shear stress on NF-κB signal transduction may be physiologically relevant in contributing to the localization of atherosclerotic lesions. It is important to note however that the complex hemodynamic flow profiles *in vivo* are virtually impossible to replicate *in vitro* and thus these studies require confirmation in animal models.

RATIONALE AND HYPOTHESIS

We are interested in mechanisms regulating atherosclerotic lesion initiation and in particular mechanisms governing the topographic distribution of lesions. Although clinically significant complications of atherosclerosis, such as plaque ulceration, rupture and thrombosis, occur in established or advanced atherosclerotic plaques, elucidation of pathogenic mechanisms of early lesion development may lead to interventions that delay or prevent lesion progression and complications.

Our goal is to further our understanding with respect to "why lesions occur in certain sites and not in other sites throughout the arterial tree", upon superimposition of systemic atherogenic stimuli.

Previous studies have shown increased LDL retention, increased expression of VCAM-1 and ICAM-1 and increased monocyte adherence in lesion prone sites. Since NF-κB may be activated by various atherogenic stimuli including low shear stress and oxLDL and in turn can regulate expression of multiple genes important in early lesion development including adhesion molecules such as VCAM-1, we set out to examine the role of NF-κB signal transduction in the localization of atherosclerotic lesions.

Although the extent of lesion formation can be quite variable, even in inbred strains of mice, their topographic distribution is highly reproducible, particularly in the ascending aorta and aortic arch. Our approach was to first map regions in the mouse ascending aorta and arch predisposed to and protected from lesion formation. The expression and activation of key endothelial cell NF-κB components were then compared in predisposed vs. protected regions, both under control and stimulated conditions. We chose to exclusively examine the endothelial cell monolayer, since endothelial cell dysfunction is a hallmark of early lesion formation and shear stress gradients have the greatest and most direct influence on endothelial cells.

Although numerous studies have suggested a correlation between NF-κB signal transduction and atherogenesis, the majority have been *in vitro* and therefore may lack physiological relevance. To date, only one study has shown NF-κB activation in advanced human plaques. Thus, our study is the first to examine NF-κB signal transduction ex vivo, in the context of lesion initiation and the topographic distribution of lesions. This study contributes valuable and novel insight as to how diverse atherogenic stimuli may converge on a signal transduction pathway to coordinate the expression of several genes important in early lesion development.

HYPOTHESIS:

Endothelial cell NF-κB signal transduction contributes to the localization of atherosclerotic lesions

CHAPTER 2

Development of a mouse model to examine gene expression in regions with high and low probability for atherosclerotic lesion formation

OBJECTIVES:

1) Aortic dissection – In our lab we have previously observed highly reproducible lesions in certain regions of the mouse ascending aorta and aortic arch. The first objective was to develop a reproducible dissection procedure which would allow the aortic tissue to lie flat on a slide, permitting *en face* analysis. Anatomic landmarks were also established.
2) Oil red O staining – After the aortas were opened, the goal was to visually determine regions with and without lesions. Oil red O (which stains lipid) was used as a lesion marker to stain aortas after feeding a high cholesterol diet.
3) Probability Mapping – To develop probability maps for lesion formation based on the oil red O stained aortas in order to assess gene expression in high and low probability regions (HP and LP), prior to lesion formation.
4) Locating HP and LP regions – The goal was to perform *en face* analysis under the confocal microscope, and develop a procedure to locate HP and LP fields under the microscope, based on the probability maps.

MATERIALS AND METHODS:

Animals and Diets

Mice were maintained in accordance with guidelines of the Canadian Council on Animal Care. Male and female C57BL/6 and LDLR -/- mice (crossed 10 times into the C57BL/6 strain) were purchased from Jackson Laboratory. At 2 to 4 months of age, they were fed standard chow or a cholate-free AIN-76A semipurified diet containing high fat (40% of energy intake) and 1.25% cholesterol (diet D12108, Research Diets, Inc (80)) for 4 or 12 weeks.

Harvesting of Mouse Aortas

The arterial tree of halothane–anesthetized mice was perfused via the left ventricle. PBS (pH 7.4) was infused for 5 minutes then 10% formaldehyde for 15 minutes and PBS for 5 minutes. The perfusion pressure was maintained at 100 mm Hg with a pressurized gas cylinder and regulator. The ascending aorta and aortic arch were harvested, and periaortic adipose tissue dissected while immersed in cold PBS.

Aortic dissection

After perfusion fixation and dissection of periaortic adipose tissue, the aorta was opened in a reproducible manner using 3 anatomic landmarks as guides under a dissecting microscope (Figure 3). The cuts were made in the following order:

a) vertical cut at proximal end of left common carotid artery and triangular notch where the vertical cut intersects the lesser curvature of the aortic arch (C)
b) removal of brachiocephalic trunk and cut along greater curvature from the commissure of the right and posterior aortic valve leaflets
c) 2 triangular notches at the commissures of the aortic valves (A and B)

FIGURE 3 - Dissection of the ascending aorta and aortic arch. The aorta is opened using anatomic landmarks A, B and C (B is on the posterior aspect of the aorta and is not visible in the upper panel). Dashed lines indicate cuts. The lower panel shows the *en face* view of the dissected proximal aorta. Small notches at the commissures of the aortic valve (A and B) and at the midpoint of the lesser curvature (C), correspond to the anatomic landmarks in the upper panel.

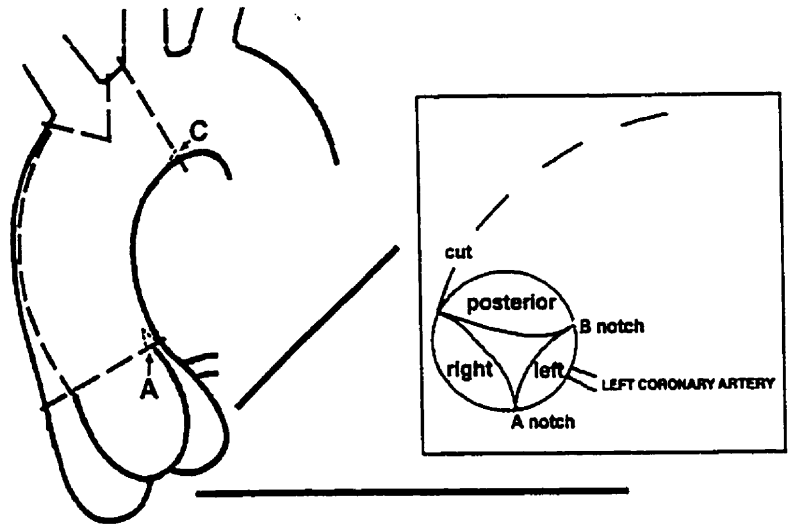
C
A
cut
posterior
B notch
right
left
LEFT CORONARY ARTERY
A notch

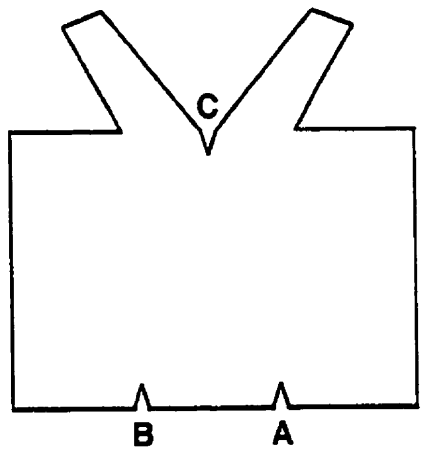
C
B
A

Oil red O staining

To determine sites where lesions initially develop, 8 LDLR -/- mice were fed a semipurified, 1.25% cholesterol, cholate-free diet for 4 weeks. Aortas were harvested, opened as described above and stained with oil red O. The oil red O stained aortas were mounted *en face* with glycerol on glass slides and stored at 4 ^{0}C. To determine sites protected from lesion formation, 8 LDLR -/- mice were fed the cholesterol - enriched diet for 12 weeks and stained with oil red O.

Probability Mapping

En face oil red O-stained aortas were photographed and scanned into a computer. Using image analysis software (C-imaging), a rectangle was defined for each aorta using landmarks A and B for width and C for height. Each rectangle was transformed into a standard size and overlaid with a grid (560 squares). Squares in the grid were scored for presence or absence of oil red O stain which is red in colour. For each group (4 wk and 12 wk cholesterol diet) the 8 grids were compiled to produce a final grid with each square containing a number between 0 (no samples contained red) and 8 (all samples contained red). From these final grids 2 probability maps were constructed for lesion development with respect to landmarks A, B and C.

Locating HP and LP regions under the confocal microscope

The probability maps outlined a region that was predisposed to lesion formation and an adjacent region that was protected (see results). In order to assess expression of genes in HP vs LP regions we devised a method to locate three fields in each region using the anatomic landmarks A, B and C. The procedure is as follows:

1) Points A, B and C are brought sequentially into the center of the field of view and micrometer readings are recorded (x,y coordinates) – A (X_A, Y_A), B(X_B, Y_B), C(X_C, Y_C)

(Note: The aorta must be positioned on the slide with points A and B parallel with the top of the slide)

2) The centroid of triangle ABC is calculated and designated as point $D(X_D, Y_D)$.

3) Based on the probability maps and using the x,y co-ordinates of points A, B, C and D we can locate 3 HP and 3 LP non-overlapping fields using the following formulae:

$HP1 = XD + .4(X_B-X_D)$

$YD + .3(Y_C-Y_D)$

$HP2 = XD + .6(X_B-X_D)$

$YD + .4(Y_C-Y_D)$

$HP3 = XD + .8(X_B-X_D)$

$YD + .6(Y_C-Y_D)$

$LP1= XA - .6(X_B-X_A)$

$YD - .56(Y_D-Y_A)$

$LP2 = XA - .65(X_B-X_A)$

$YD - .14(Y_D-Y_A)$

$LP3 = XA - .5(X_B-X_A)$

$YD - .18(Y_D-Y_A)$

Silver nitrate staining

Mouse aortas were perfused with PBS (5 mL over 1 minute), 0.25% silver nitrate dissolved in distilled water (5 mL over 30 seconds), then PBS again (2.5 mL over 15 seconds). Perfusion was via the left ventricle using 10 mL syringes. Pressure fixation followed using 2% paraformaldehyde infused for 15 minutes at 100 mm Hg. Harvested aortas were mounted on the same day and photographed using a standard light microscope.

RESULTS

Mapping of high probability (HP) and low probability (LP) regions for lesion development in LDLR -/- mice fed a cholesterol diet for 4 or 12 weeks

Studies with $LDLR^{-/-}$ mice in our laboratory revealed that the extent of atherosclerotic lesion formation is variable even amongst inbred littermates, however the location of lesions is highly reproducible, particularly in the ascending aorta and aortic arch. Figure 4 illustrates examples of ORO stained aortas after feeding a 4 week or 12 week cholesterol diet. The aortas from the 4 week diet group consistently shows lesions in the central portion of the *en face* preparation which corresponds to the lesser curvature, whereas the sides are protected. The 12 week diet group shows expansion of lesions in the central portion as compared to the 4 week diet group, although the sides remain protected. The sides remained protected even in mice fed a cholesterol rich diet for 20 weeks (data not shown).

Based on the Oil red O stained aortas probability maps were constructed with respect to landmarks A, B and C. Figure 5b shows regions with the highest probability for lesion development (>70% of mice after feeding a 4 week cholesterol diet, n=8) in the portion of the aorta corresponding to the lesser curvature. This region was designated as HP (high probability or >70% probability for lesion formation). Figure 5a shows an adjacent region (to the right of A) with low probability (LP) or 0% probability for lesion formation. These LP regions were mapped by feeding mice a cholesterol diet for 12 weeks (n=8).

Endothelial cells in the HP region have a polygonal shape and random orientation

The shape of endothelial cells is known to reflect the local hemodynamic environment (47-50, 54, 81, 82), therefore, intercellular junctions were stained with silver nitrate in order to visualize endothelium in the HP and LP regions of the mouse proximal aorta. Endothelial cells in the LP region were elongated parallel to the direction of blood flow, whereas in the HP region they were more polygonal and oriented randomly (Figure 6).

FIGURE 4 - Representative oil red O stained aortas after feeding a high cholesterol diet. 2 groups of 8 mice were fed a 1.25% cholesterol diet for 4 or 12 weeks. Oil red O stained *en face* preparations were used to map high and low probability (HP and LP) regions for lesion development.

IDENTIFICATION OF HIGH AND LOW PROBABILITY REGIONS FOR ATHEROSCLEROTIC LESION DEVELOPMENT

OIL RED O STAINING OF C57BL/6 ASCENDING AORTAS HIGH CHOLESTEROL DIET

4 weeks

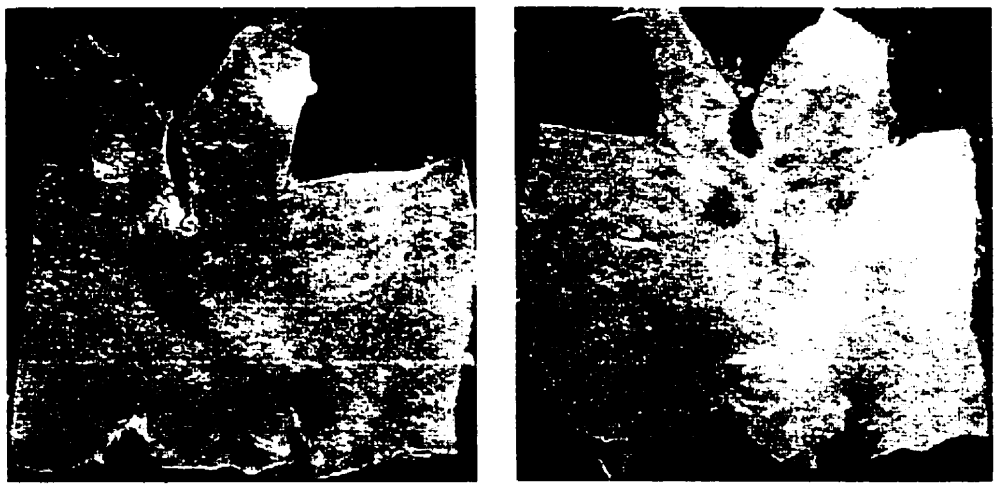

12 weeks

FIGURE 5 - Mapping of HP and LP regions in 8 $LDLR^{-/-}$ mice fed a cholesterol diet for 12 weeks with respect to anatomic landmarks A, B and C. a) Regions that were stained with oil red O in all mice (100%) or had absent staining (0%) are indicated. The LP regions remained lesion free in mice fed a cholesterol diet for 20 weeks (not shown). b) Oil red O staining of the central portion of aortas from $LDLR^{-/-}$ mice fed cholesterol diet for 4 weeks was used to define regions with the highest probability for lesion development (staining in >70% of mice, n=8). c) *En face* view showing HP and LP regions.

a

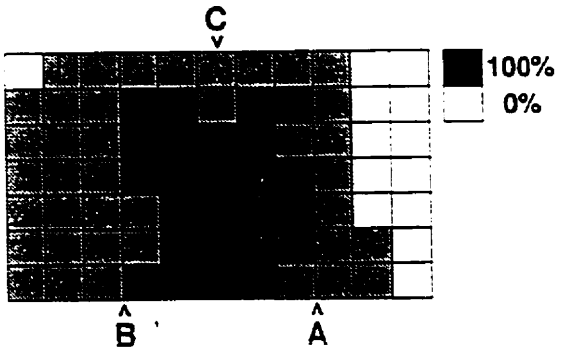

b

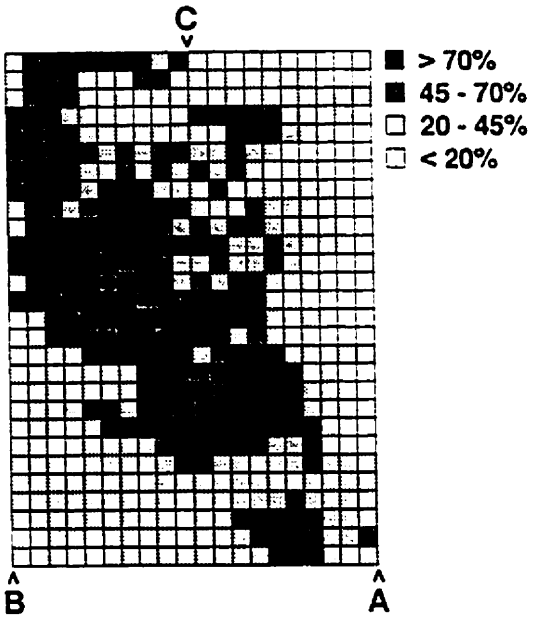

c

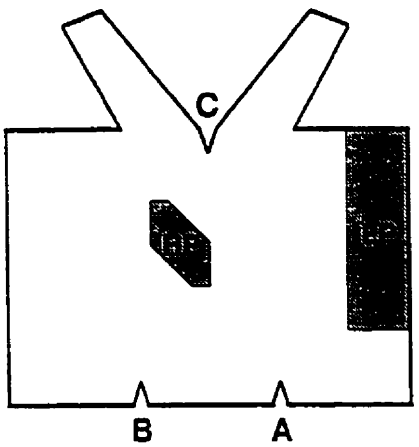

Figure 6 - Silver nitrate staining in HP and LP regions. Representative images were obtained from a C57BL/6 mouse aorta. Endothelial cells in the HP region have variable shape and random orientation, whereas in the LP region they are elongated and aligned in the direction of blood flow (left to right).

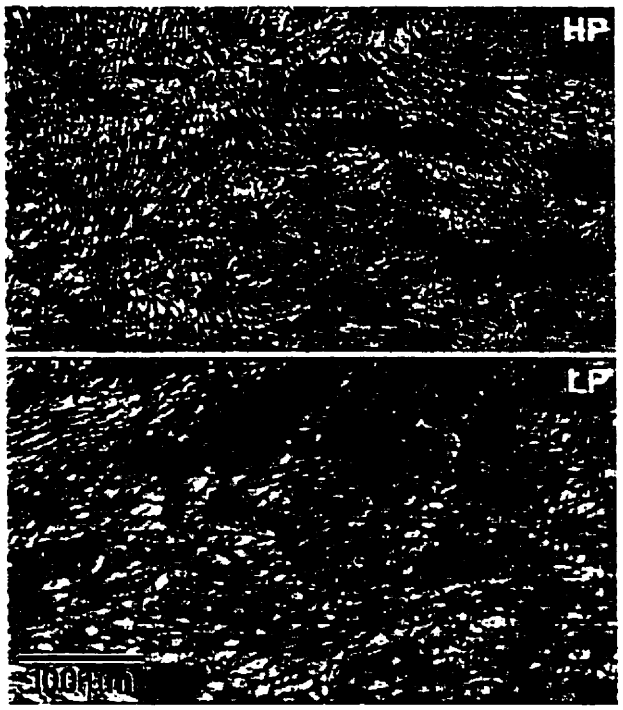
HP
LP
100μm

Fluorescent staining with propidium iodide or Sytox demonstrated that endothelial nuclei in the LP region were oval, parallel to the direction of blood flow and uniformly spaced. In the HP region, they were irregular and appeared to be at a higher density (Figures 8-11). These observations suggested that significantly different local hemodynamics forces were exerted on endothelium at HP and LP regions of the ascending mouse aorta.

CHAPTER 3

Immunofluorescent examination of key endothelial cell NF-κB components in HP vs. LP regions

OBJECTIVES:

1) Expression of NF-κB components –The first aim was to compare expression of key endothelial cell NF-κB components (p65, IκBα and IκBβ) in HP vs. LP regions in control or unstimulated C57BL/6 mice.
2) NF-κB activation in control mice – The goal was to determine NF-κB activation (as assessed primarily by p65 nuclear translocation) in HP vs. LP regions in control mice.
3) p65 activation after stimulation – The goal was to determine p65 nuclear translocation after stimulation with LPS or an atherogenic diet in HP vs. LP regions and compare these data with control (unstimulated) conditions.
4) Expression of NF-κB target genes – To determine expression of genes important in early lesion development and regulated by NF-κB in HP vs. LP regions
5) Expression of control genes – To determine expression of genes constitutively expressed by endothelial cells and not regulated by NF-κB in HP vs. LP regions.

HYPOTHESIS: The NF-κB signal transduction pathway is primed for activation in HP region endothelial cells.

MATERIALS AND METHODS

Immunofluorescence staining reagents and protocols

Polyclonal and monoclonal primary antibodies were used. Polyclonal antibodies to NF-κB and IκB peptides were purchased from Santa Cruz Biotechnology, Inc., as purified IgG. They included goat anti-p65 (C-20, 20 C-terminal amino acids) (sc-372-G. 1:500 dilution), goat anti-IκBα (C-21) (sc-371-G, 1:400 dilution), rabbit anti-IκBβ (S-20) (sc-946, 1:200 dilution). Phospho-IκBα (Ser32) polyclonal rabbit antibody was purchased from New England Biolabs, Inc. and used at a 1:20,000 dilution. This antibody reacts with IκBα only when serine 32 is phosphorylated. Other antibodies included monoclonal rat anti-mouse E-selectin IgG2a (PharMingen, 1:500 dilution), monoclonal rat anti-mouse ICAM-2 IgG2a (PharMingen, 1:200 dilution), monoclonal rat anti-mouse VCAM-1 (M/K-2.7, American Type Culture Collection, IgG1, undiluted tissue culture supernatant), polyclonal goat anti-mouse PECAM-1 (M-20, sc-1506, Santa Cruz, 1:200 dilution).

Negative controls included nonimmune goat, rabbit or rat IgG (Jackson Immuno Research Labs, Inc., same species and dilution as the primary antibody). For anti-p65, the primary antibody was incubated with blocking peptide-immunogen (sc-372P, Santa Cruz, 1:50 dilution). Secondary antibodies included biotin-conjugated donkey polyclonal anti-goat, rabbit or rat IgG (Jackson) or Cy3-labeled donkey anti-goat or anti rat.

The immunostaining protocol varied depending on the antibody. Tyramide signal amplification (NEN Scientific) was used for detection of p65, IκBα, IκBβ, phospho-IκBα, E-selectin and ICAM-2. Endogenous peroxidase activity was blocked by incubating aortas with 3% hydrogen peroxide in PBS (10 minutes). Tissues were permeabilized with 0.2% Triton X-100 in PBS (5 minutes) and blocked with Tris-HCl blocking buffer (NEN, 30 minutes). For p65, IκBα, IκBβ and ICAM-2 primary antibody incubations were for 1 hour at 22°C. For E-selectin and phospho-IκBα primary antibody incubations were overnight at 4°C. Subsequent steps included biotin-conjugated polyclonal secondary antibodies (30

minutes), steptavidin-conjugated horse radish peroxidase (30 minutes) and tyramide complexes conjugated with FITC or Cy3 for IκBβ (8 minutes). All antibodies were diluted in Tris-HCl blocking buffer (NEN) and washes between steps used Tris-HCl washing buffer (0.1M Tris-HCl pH 7.5, 0.15M NaCl, 0.05% TWEEN 20). Nuclei were counterstained with Propidium Iodide (Molecular Probes, Inc., 1:1000 dilution, 30 minutes) for FITC-tyramide or green nucleic acid stain (Sytox, Molecular Probes, 1:100 dilution, 30 minutes) for Cy3-tyramide.

Fluorescent-labeled secondary antibodies were used to detect VCAM-1 and PECAM-1 expression. Aortic cells were permeabilized with 0.2% Triton X-100 (5 minutes) and blocked with 33% donkey serum in PBS (Jackson Labs). The primary antibody to PECAM-1 was incubated for 1 hr at 22°C, whereas an overnight incubation at 4°C was used for anti-VCAM-1. The secondary antibodies were Cy3-labeled donkey anti-goat or anti rat (1:200 dilution, 30 minutes, 22°C). Aortas were washed 3 times with PBS after antibody incubations. Nuclei were counterstained with Sytox.

Aortic segments were opened and mounted using Vectashield mounting medium (Vector Labs). In each case, the distal arch served as a negative control and was incubated with nonimmune IgG from the same species as the primary antibody or primary antibody with p65 blocking peptide.

Confocal microscopy

The ascending aorta/proximal arch was opened as described previously, as was the distal arch. They were mounted on glass microscope slides using Vectashield mounting medium (Vector Laboratories) with the endothelium facing up. Images of the endothelial cell monolayer were obtained using a Bio-Rad MRC-1024ES confocal microscope equipped with a krypton/argon laser and a 60x 1.4-numerical aperture objective (Nikon). HP and LP regions were located using 3 anatomic landmarks as reference points. In every mouse, 3 or 4 images were obtained from each HP and LP region. An HP region was sampled first and was used to optimize the confocal settings, which were maintained for other images,

including the negative control (distal arch). The distribution and intensity of fluorescence were quantified for each antibody using the confocal software frequency histogram function. For each mouse, the negative control was used to establish a pixel intensity that eliminated 99% of the background signal. Background fluorescence was then subtracted by applying this threshold to all HP and LP images, and the percent pixels with remaining signal and the average signal intensity were recorded for each image.

Statistical analyses

Differences among treatment groups were evaluated using a one-way analysis of variance. Within each treatment group, a paired t-test was used to determine differences between HP and LP regions.

RESULTS

High expression levels of p65, IκBα and IκBβ in the HP region of untreated standard chow-fed mice.

A polyclonal antibody that recognizes p65 in the cytoplasm of resting cells when complexed to IκBs, as well as translocated to the nucleus upon activation of NF-κB was used. In initial experiments, the specificity of immunostaining of mouse aortic endothelium with the anti-p65 antibody was demonstrated. This showed that inclusion of the blocking peptide (immunogen) during incubations with primary antibody completely inhibited staining (Figure 7).

Subsequent studies evaluated HP and LP regions in the ascending aorta and proximal arch of untreated standard chow-fed C57BL/6 and $LDLR^{-/-}$ mice. Expression of p65, IκBα and IκBβ was detected in LP region, however much higher levels were found in endothelium of the HP region (Figure 8). In terms of the percent positive pixels, expression in the HP region was 5 to 18-fold greater than that in the LP region (Table 1). The vast majority of staining for all three proteins was cytoplasmic. In a minority (12%) of endothelial cells of the HP region, p65 staining was found in the nucleus (Table 2) and consisted of confluent areas covering a portion of the nucleus or complete nuclear covering. In the LP region, nuclear p65 staining was very infrequent (<3%) and covered only a fraction of the nucleus. Significant differences in p65 nuclear translocation were not found between wild type C57BL/6 and $LDLR^{-/-}$ mice fed standard lab chow and these data were combined in Table 2.

The absence of abundant NF-κB activation in HP and LP regions of untreated mice was confirmed by staining with an antibody specific for IκBα phosphorylated at serine32. Weak cytoplasmic staining was detected as occasional discrete cytoplasmic aggregates (Figure 9b). Phospho-IκBα staining was more abundant in the HP region (Table 2), which is consistent with our p65 nuclear translocation data.

FIGURE 7 - Specificity of p65 immunostaining in aortic endothelial cells. Confocal images of random segments of the descending thoracic aorta from control (a and b) and 100 μg LPS-treated (c and d) mice stained for p65 (green). Nuclei were counterstained with propidium iodide (red). In control mice (a), p65 was detected in cytoplasm, whereas in LPS-treated mice (c), staining was in the nucleus. Yellow represents colocalized green and red fluorescence. Both cytoplasmic and nuclear staining for p65 in control and LPS-treated mice was inhibited by inclusion of a blocking peptide during incubation with the primary antibody (b and d).

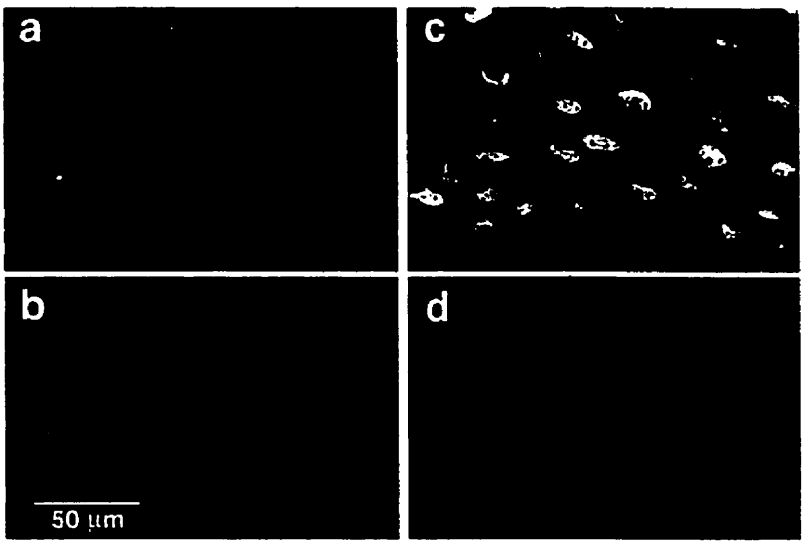
a
c
b
d
50 µm

FIGURE 8 - High expression levels of p65, IκBα and IκBβ in the HP region of untreated standard chow-fed C57BL/6 mice. For each antibody, representative confocal images of HP and LP regions obtained from the same mouse are shown (p65 and IκBα - green and IκBβ - red fluorescence).

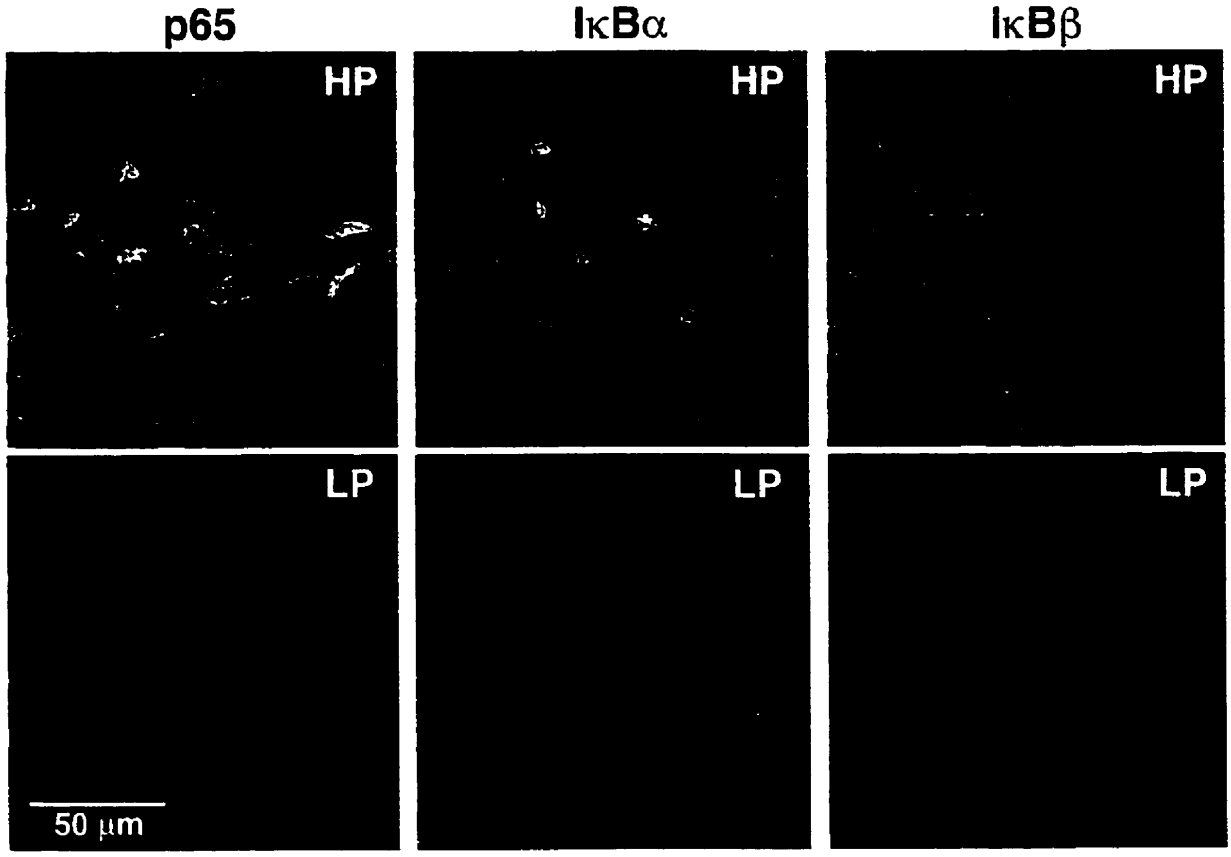
p65
IκBα
IκBβ
HP
HP
HP
LP
LP
LP
50 μm

Table 1: Quantification of endothelial cell p65, IκBα and IκBβ expression in HP and LP regions of mouse ascending aorta and proximal arch by immunoconfocal microscopy .

Antigen	Genotype [A]	n [B]	% Positive Pixels		p [C]	Average Pixel Intensity		p [C]
			HP region	LP region		HP region	LP region	
p65	$LDLR^{+/+}$	5	48.0 ± 17.4	4.9 ± 7.3	< 0.001	113.3 ± 30.4	62.1 ± 26.4	< 0.01
p65	$LDLR^{-/-}$	5	31.2 ± 12.9	2.2 ± 1.4	< 0.01	103.9 ± 10.9	69.0 ± 7.2	< 0.05
IκBα	$LDLR^{+/+}$	5	17.8 ± 8.9	0.9 ± 0.7	< 0.05	116.6 ± 30.9	96.0 ± 25.8	< 0.05
IκBβ	$LDLR^{+/+}$	5	39.7 ± 3.2	8.1 ± 4.6	< 0.001	87.4 ± 2.3	71.9 ± 13.3	< 0.05

[A] all mice were in the C57BL/6 background and were fed standard chow

[B] n represents the number of mice (3 or 4 images were obtained in each HP and LP region of every mouse)

[C] paired t-test (HP - LP)

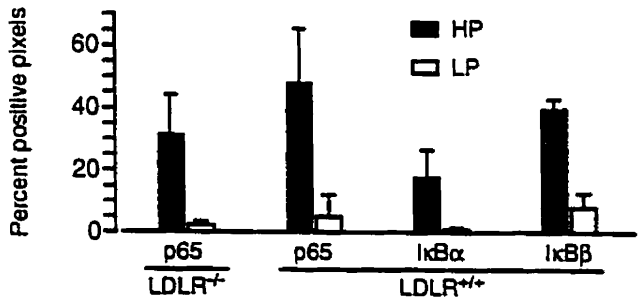

This histrogram represents the above data in graphical form

Table 2: Endothelial cell NF-κB activation in HP and LP regions of untreated C57BL/6 mice.

Criterion for NF-κB activation	n	HP Region	LP Region	p [A]
% of nuclei with translocated p65	10	12.5 ± 5.5	2.4 ± 4.4	< 0.0001
phospho-specific IκBα - % positive pixels	3	4.7 ± 1.2	0.43 ± 0.28	< 0.05

[A] paired t-test (HP - LP)

LPS treatment or feeding LDLR$^{-/-}$ mice an atherogenic diet activates NF-κB predominantly in the HP region.

The above data demonstrated that in untreated standard chow-fed mice NF-κB was activated in only a minority of endothelial cells located predominantly in the HP region. Most HP region endothelial cells contained abundant cytoplasmic p65 and IκBs, and this suggested that their NF-κB signal transduction pathway was primed for activation. If these cells encounter a stimulus that activates IκB kinases, abundant IκB substrate would be available for phosphorylation and degradation, allowing multiple molecules of p65 to translocate to the nucleus. Expression of NF-κB components was relatively low in the LP region, therefore the extent of p65 nuclear translocation and gene transactivation should be low even following a potent activation stimulus. This possibility was evaluated by injecting wild type C57BL/6 mice with LPS, or by feeding LDLR$^{-/-}$ mice with an atherogenic diet for 2 weeks.

Dose-dependent nuclear translocation of p65 was found in the HP region endothelial cells 30 minutes following administration of LPS (Figure 9a and Table 3). Staining for p65 covered virtually the entire nucleus and cytoplasmic staining was reduced or absent. In contrast, endothelial nuclei in the LP region did not show a significant increase in p65 translocation and showed only focal positive staining.

Staining for phospho-IκBα was also assessed following treatment of mice with 100 μg of LPS (Figure 9b and Table 4). LPS-treatment resulted in a 7 to 10-fold increase in cytoplasmic phospho-IκBα staining in HP and LP regions and indicated that IκB kinases were activated in both regions. These data differ from p65 nuclear translocation, which was restricted to the HP region (Table 3). The extent of phospho-IκBα staining in the LP region of LPS-treated mice was comparable to that found in the HP region of controls.

Feeding LDLR$^{-/-}$ mice an atherogenic diet (semipurified, 1.25% cholesterol, high fat cholate-free) for 2 weeks resulted in increased nuclear translocation of p65 in both the HP

FIGURE 9 - LPS treatment or feeding LDLR$^{-/-}$ mice an atherogenic diet activates NF-κB predominantly in the HP region. Representative immunoconfocal images from HP and LP regions are shown. (a) Dose dependent nuclear translocation of p65 (green) is seen in HP regions 30 minutes following i.p. injection of LPS (0, 10 or 100 μg). Nuclei are counterstained with propidium iodide. (b) Punctate green staining for phospho-IκBα (P-IκBα) is abundant in the cytoplasm of HP region endothelium following administration of 100 μg LPS. (c) Increased p65 nuclear translocation occurs in HP regions of LDLR$^{-/-}$ mice 2 weeks after ingestion of a 1.25% cholesterol-enriched diet (cholesterol) relative to standard chow-fed (chow) mice.

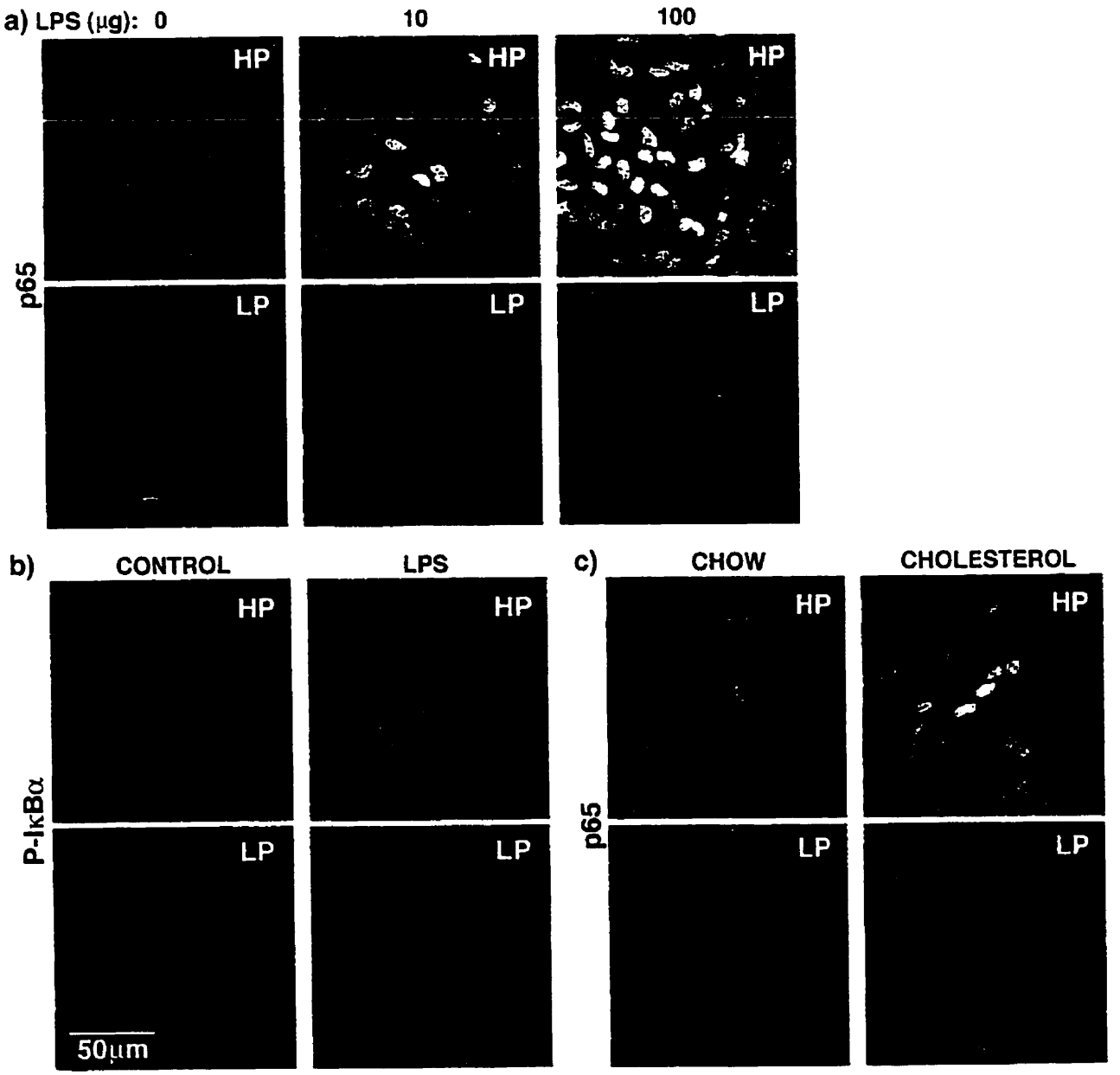
a) LPS (µg): 0
10
100
HP
LP
p65
b)
CONTROL
LPS
P-IκBα
50µm
c)
CHOW
CHOLESTEROL

Table 3: Endothelial cell NF-κB activation in HP and LP regions induced by LPS treatment or feeding a 1.25% cholesterol diet.

Treatment	Genotype	n	% of nuclei with translocated p65		p [A]
			HP region	LP region	
LPS (0 μg)	$LDLR^{+/+}$	5	12.2 ± 6.1	3.6 ± 6.1	< 0.01
LPS (10 μg)	$LDLR^{+/+}$	4	40.1 ± 11.0 [B]	3.1 ± 2.6	< 0.01
LPS (100 μg)	$LDLR^{+/+}$	3	88.0 ± 6.1 [B,C]	3.7 ± 2.9	< 0.005
Standard chow	$LDLR^{-/-}$	5	12.8 ± 5.1	1.0 ± 1.2	< 0.01
Cholesterol diet (2 wks)	$LDLR^{-/-}$	5	22.8 ± 5.5 [B]	2.7 ± 0.8 [C]	< 0.005

[A] paired t-test (HP - LP)

[B] $p < 0.05$ versus 0 μg LPS or standard chow

[C] $p < 0.05$ versus 10 μg LPS

Table 4: Endothelial cell NF-κB activation in HP and LP regions following LPS treatment, determined by staining with polyclonal phospho-specific IκBα antibody.

Treatment	n	% Positive Pixels		p [A]	Average Pixel Intensity		p [A]
		HP region	LP region		HP region	LP region	
LPS (0 μg)	3	4.7 ± 1.2	0.43 ± 0.28	< 0.05	60.1 ± 12.4	52.1 ± 3.9	
LPS (100 μg)	4	32.8 ± 7.6 [B]	4.4 ± 2.9 [B]	< 0.01	62.7 ± 1.8	53.6 ± 4.0	< 0.05

[A] paired t-test (HP - LP)

[B] $p < 0.05$ versus 0 μg LPS

and LP areas relative to mice receiving standard lab chow (Figure 9c and Table 3). The extent of nuclear translocation in the LP region of cholesterol-fed mice was several fold lower than that found in the HP region of control mice (Table 3).

Expression of NF-κB target genes is preferentially upregulated by LPS in the HP region

The expression of VCAM-1 and E-selectin, genes whose induced expression is dependent on NF-κB activation (70), was compared in HP and LP regions of control and LPS-treated mice (Figure 10 and Table 5). Aortas from C57BL/6 mice were harvested 5 or 6 hours after LPS injection for E-selectin and VCAM-1, respectively, and immunostaining was carried out on triton X-100 permeabilized endothelium. In untreated mice, VCAM-1 was expressed preferentially in the HP region, whereas E-selectin expression was not detected (Table 5). Treatment with 10 or 100 μg of LPS induced dose-dependent expression of both genes. VCAM-1 expression increased 2 and 4 fold in the HP region, however in the LP region, increased expression was not observed following the 10 μg dose and only a modest increase was found in response to 100 μg of LPS. The expression level of VCAM-1 induced by the 100 μg dose of LPS in the LP region did not approach that found in the HP region of control mice (Table 5). This was analogous to the p65 nuclear translocation data. (Table 3). LPS-induced E-selectin expression was pronounced in the HP region, whereas it was modest in the LP region (Table 5).

Expression of control genes is comparable in HP and LP regions

PECAM-1 and ICAM-2 were selected as negative controls for the above experiments, because these genes are constitutively expressed by endothelial cells, their expression is not upregulated by LPS or cytokines (83, 84) and is thought to be independent of NF-κB activation. The expression levels of PECAM-1 and ICAM-2 in HP and LP regions was comparable in untreated mice and was not altered 12 hours after a 100 μg LPS

FIGURE 10 - Expression of NF-κB target genes is preferentially upregulated by LPS in HP region endothelium. Representative immunoconfocal images of permeabilized endothelium illustrate LPS dose-dependent increased VCAM-1 (red) and E-selectin (green) expression. The magnitude of expression is significantly greater in HP regions. In control mice (0 μg LPS), VCAM-1, but not E-selectin, expression is detected in the HP region.

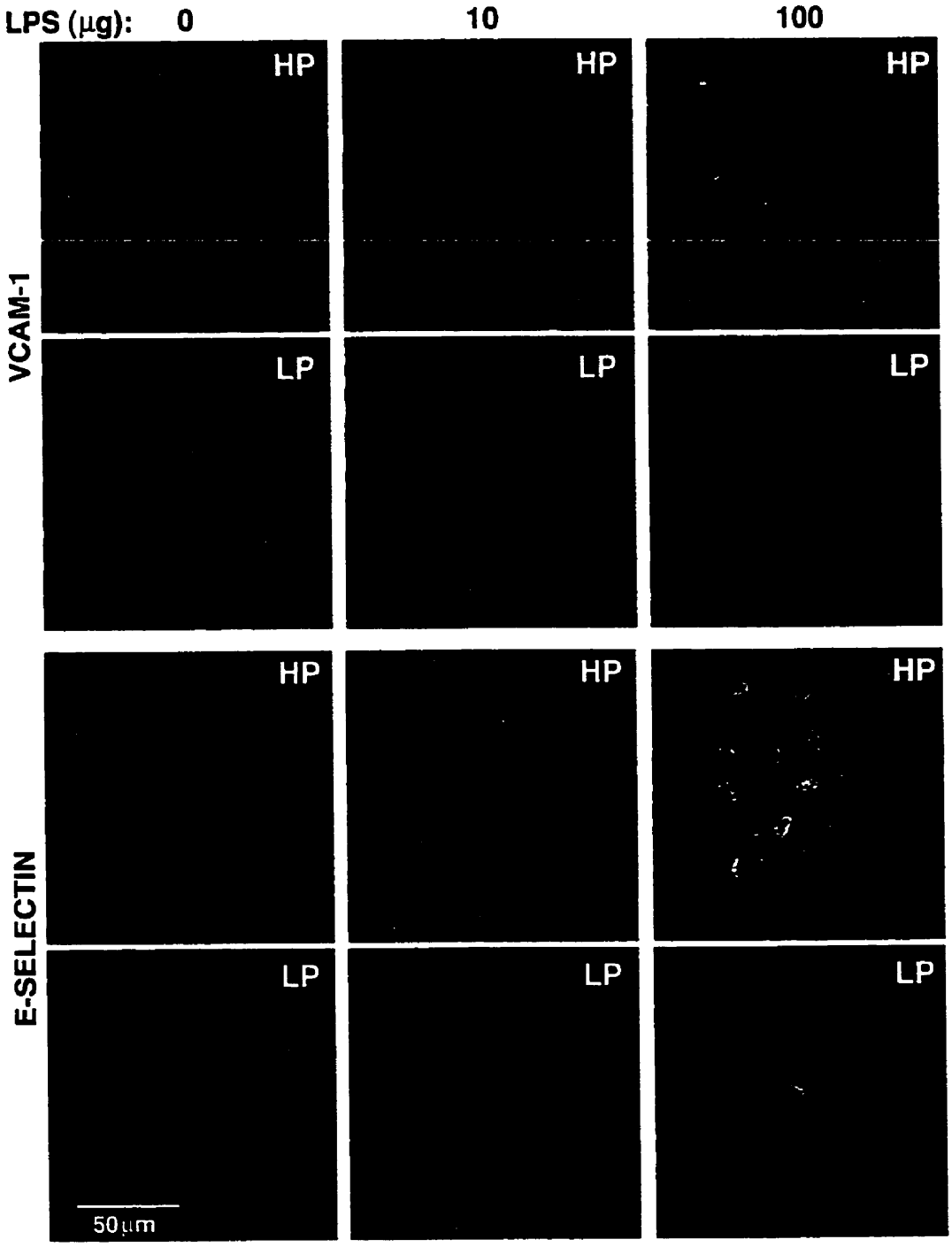
LPS (μg): 0
10
100
VCAM-1
E-SELECTIN
HP
LP
50μm

FIGURE 11 - Expression of PECAM-1 (CD 31) and ICAM-2 in HP and LP regions. Representative immunoconfocal images of permeabilized endothelium illustrate that expression of PECAM-1 and ICAM-2 is abundant in control mice and not inducible by LPS. PECAM-1 staining (red) is localized to endothelial junctions in the HP region, whereas in the LP region, it is more diffuse. ICAM-2 staining (green) is comparable in HP and LP regions. The irregular shape and orientation of endothelium of the HP region is illustrated by PECAM-1 staining.

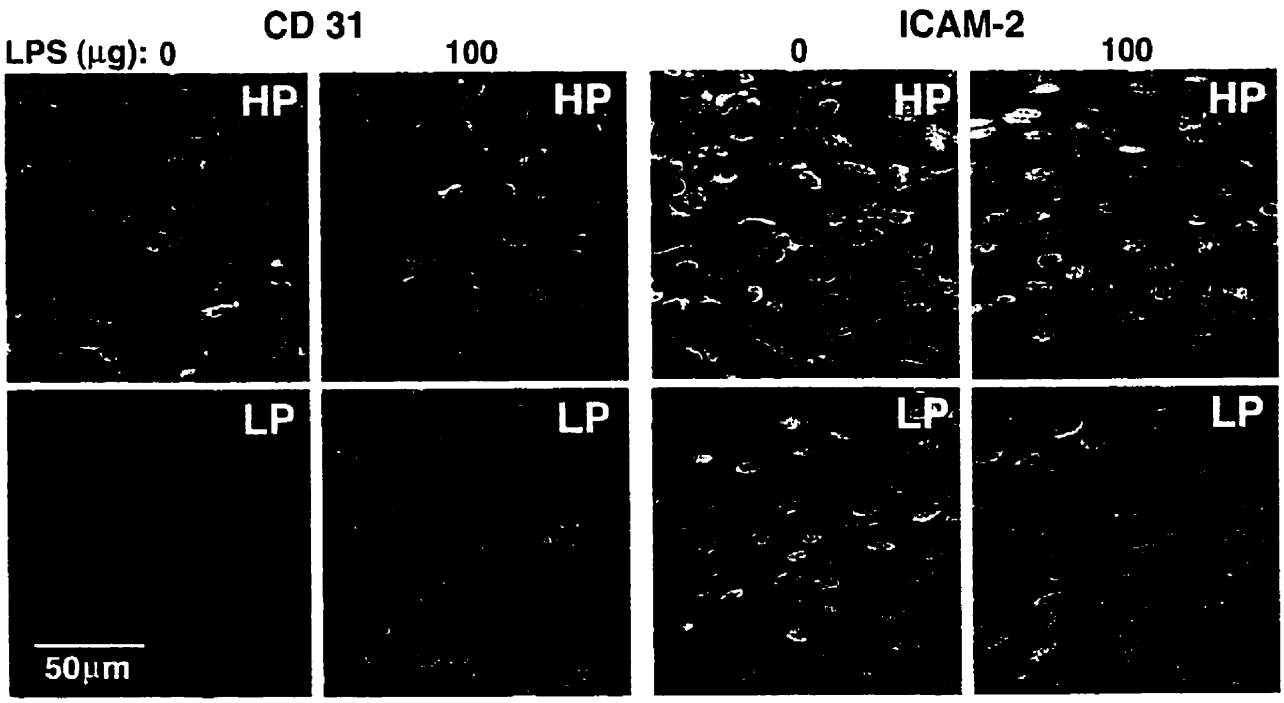
CD 31
ICAM-2
LPS (μg): 0
100
0
100
HP
HP
HP
HP
LP
LP
LP
LP
50μm

Table 5: Expression of VCAM-1, E-selectin, PECAM-1 and ICAM-2 detected by immuno-confocal microscopy in endothelial cells of HP and LP regions of the proximal mouse aorta.

Antigen	LPS	n	% Positive Pixels		p [A]	Average Pixel Intensity		p [A]
	(µg ip)		HP region	LP region		HP region	LP region	
VCAM-1	0	5	10.0 ± 4.9	1.6 ± 1.2	< 0.05	63.9 ± 6.3	57.6 ± 7.4	< 0.05
VCAM-1	10	3	22.2 ± 7.9	1.5 ± 1.6	< 0.05	73.9 ± 7.1	59.9 ± 6.4	< 0.05
VCAM-1	100	3	43.1 ± 14.1	4.9 ± 4.9	< 0.05	82.6 ± 4.7	60.9 ± 3.5	< 0.05
E-selectin	0	3	0	0		0	0	
E-selectin	10	3	12.2 ± 8.7	3.1 ± 3.5	< 0.05	91.4 ± 12.0	79.0 ± 4.5	
E-selectin	100	3	59.7 ± 11.9	4.1 ± 1.9	< 0.05	127.5 ± 7.3	87.4 ± 19.0	< 0.05
PECAM-1	0	5	49.3 ± 25.0	27.7 ± 14.2		116.8 ± 18.5	89.0 ± 20.4	< 0.05
PECAM-1	100	5	57.2 ± 20.2	43.1 ± 27.6		106.7 ± 17.7	79.1 ± 16.5	< 0.05
ICAM-2	0	5	95.5 ± 8.9	96.2 ± 5.5		180.2 ± 44.1	170.3 ± 30.5	
ICAM-2	100	3	96.6 ± 2.2	92.5 ± 8.9		185.3 ± 20.1	160.5 ± 40.2	

[A] paired t-test (HP - LP)

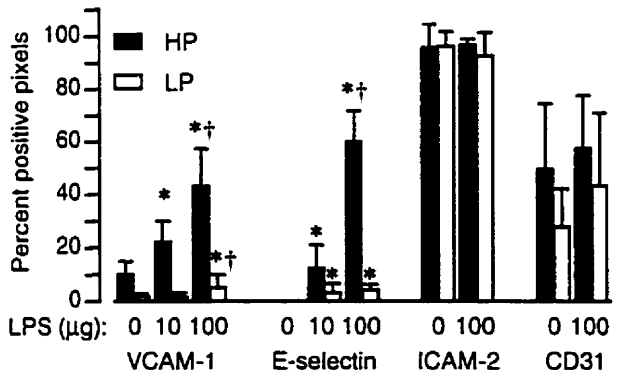

This histogram is a graphical representation of the above data. There are significant differences ($p<0.05$, paired t-test) between HP and LP regions for VCAM-1 and E-selectin, but not ICAM-2 and PECAM-1. Significant differences from 0 and 10 µg LPS groups are denoted by * and †, respectively (ANOVA).

injection (Figure 11 and Table 5). The localization of PECAM-1 within endothelial cells differed in HP and LP regions. PECAM-1 was predominantly at intercellular junctions of HP region endothelial cells and in LP endothelium, it was also distributed throughout the cytoplasm. This distribution pattern was not affected by LPS treatment (Figure 10). ICAM-2 localization was similar in HP and LP regions.

CHAPTER 4

DISCUSSION

This study evaluated the expression and activation of key endothelial cell NF-κB/IκB components in regions of mouse aorta predisposed to and protected from atherosclerotic lesion formation. The HP and LP regions were located in the lesser and greater curvatures, respectively, of the ascending aorta and proximal arch, which permitted meaningful comparison of fluorescent signal intensities following immunostaining of the entire aortic segment. This *ex vivo* analysis is valuable because it is difficult, if not impossible, to replicate in cell culture models all of the factors that promote atherosclerosis at HP regions *in vivo*. These include complex hemodynamic profiles influenced by a pulsatile component of the cardiac cycle and elasticity of the artery wall, local differences in extracellular matrix and influences from adjacent smooth muscle cells or adherent/transmigrating leukocytes. The data from control and cholesterol-fed mice represent steady-state levels of NF-κB/IκB protein expression and NF-κB activation, whereas *in vitro* studies usually model acute alterations in hemodynamics (85) and even "chronic" studies are limited to 24 or 48 hours. The minute size of HP and LP regions of the mouse ascending aorta and arch necessitated an immunohistochemistry-based approach and precluded biochemical analyses.

The endothelial cells in the HP region had random orientation and variable shapes, including polygonal. In contrast, LP region endothelial cells were uniformly elongated and aligned in the direction of blood flow. This finding is consistent with endothelium in HP and LP regions being exposed to disturbed and unidirectional, laminar hemodynamic forces, respectively. Previous studies reported similar cell shapes after exposure of endothelial cells to disturbed or unidirectional, laminar flow (41, 54, 86). The polygonal shape of endothelial cells also occurs when shear stresses are very low (54), but this is unlikely to be the case in the aortic arch.

Acute exposure of endothelium to laminar shear stress can activate various signal transduction cascades and lead to alterations in expression levels of numerous genes (87).

After endothelial cells become acclimatized to an alteration in laminar shear forces, these signaling cascades are downregulated. *In vivo* most vascular endothelial cells, including those in arterial regions with low predisposition to atherosclerosis, are chronically exposed to laminar shear forces, which is their physiological milieu. Chronic exposure to laminar shear stress may upregulate the expression of unique genes that are atheroprotective (88, 89), or may promote mechanisms that actively repress expression of broad categories of genes. Several groups have demonstrated that surgically introduced alterations in fluid dynamics in conjunction with hypercholesterolemia influences atherosclerotic lesion formation (37, 38), which further supports the role of hemodynamics in lesion development.

In endothelial cells, the main form of NF-κB with transactivation potential is p65, and in resting cells it is associated predominantly with IκBα and IκBβ (58). In endothelium of control mice, expression levels of p65, IκBα and IκBβ were 5-18 fold higher in the HP versus the LP region. The mechanism for this is unknown, but a difference in hemodynamics in HP and LP regions is a likely factor. The extent of NF-κB activation in control mice, determined by nuclear translocation of p65 and phospho-IκBα staining, was significantly greater in the HP versus the LP region. Only partial nuclear translocation of p65 was found in less than 15% of endothelial cells of the HP region, and many cells had abundant p65 remaining in the cytoplasm presumably bound to IκBs. This suggested that hemodynamic factors do not provide a critical activation signal under control conditions, although they may be responsible for the different expression levels of NF-κB/IκB components in the two regions. Because endothelium in the HP region of control mice had abundant cytoplasmic p65 and IκBs, we propose that the NF-κB signal transduction pathway in these cells is primed to respond to activation stimuli. IκBs would be a readily available substrate for phosphorylation upon activation of IκB kinases and abundant p65 would translocate to the nucleus and transactivate gene expression.

LPS treatment or feeding $LDLR^{-/-}$ mice an atherogenic diet for 2 weeks was used to compare the extent of NF-κB activation in HP and LP regions of the mouse aorta. NF-κB

activation has been reported in advanced human atherosclerotic lesions (75), but activation in endothelium of early lesions and prior to lesion formation has not been evaluated. Feeding LDLR$^{-/-}$ mice a cholesterol-enriched diet models an important systemic risk factor and reproducibly produces atherosclerotic lesions. Based on studies that demonstrated increased lipoprotein retention at atherosclerosis-prone sites (90), it is possible that an atherogenic diet could provide preferential activation signals in the HP region. LPS, an agent known to activate NF-κB in a variety of cells (56, 57), was used to provide an acute systemic activation stimulus in both HP and LP regions. Although the contribution to atherogenesis of such an acute systemic activation of endothelium is not known, inflammatory mediators produced by acute or chronic infections are thought to modulate the development and complications of atherosclerotic lesions (91).

LPS treatment resulted in 6 to 10 fold increased phospho-IκBα staining in both HP and LP regions. This suggests that IκB kinases were activated comparably. The lower levels of phospho-IκBα in the LP region can be explained by the lower content of IκBα in these cells. LPS induced a significant and dose-dependent nuclear translocation of p65 in endothelium of the HP region, which was consistent with elevated phospho-IκBα staining. In the LP region, p65 nuclear translocation was low under all conditions. The lack of a small increase in p65 translocation in the LP region induced by LPS may reflect control of nuclear translocation in the LP region. Alternatively it may have been an experimental artifact, because the accuracy of quantifying low level p65 fluorescent signals is diminished as a result of background autofluorescence from the internal elastic lamina. This may explain the high variability between control group (0 μg LPS) mice. The mean value of this group was higher than that of LDLR$^{-/-}$ mice fed standard lab chow. Overall, the LPS studies showed that the relatively high levels of NF-κB/IκB components in the HP region were functionally quite responsive, whereas the NF-κB signal transduction pathway in the LP region was largely quiescent.

Feeding LDLR$^{-/-}$ mice a cholesterol-enriched diet for 2 weeks resulted in

approximately a 2-fold increase in p65 nuclear translocation in the HP region as compared to control mice. At this time point, ORO-stainable lesions had not developed in the HP region, but it is possible that occasional monocytes began accumulating in the intima. In the LP region, a significant increase in p65 nuclear translocation was observed also. These data suggest that hypercholesterolemia provides an activation stimulus that is not restricted to regions predisposed to atherosclerotic lesion formation and are consistent with a study by Calara et al (92). These investigators injected rats with a single bolus of human LDL and demonstrated its accumulation and oxidation throughout the aorta, associated with NF-κB activation and upregulation of ICAM-1 expression in endothelium. It is interesting to note that cholesterol feeding did not increase the expression levels of p65 or IκBs. In the LP region of cholesterol-fed $LDLR^{-/-}$ mice, the extent of endothelial cell p65 nuclear translocation was 4 to 5 fold lower than that found in the HP region of standard chow-fed $LDLR^{-/-}$ mice (2.7% versus 12.8% of nuclei). This suggests that the magnitude of NF-κB activation in aortic endothelium depends on the expression levels of NF-κB/IκB components.

The functional consequences of NF-κB activation were assessed by evaluating the expression of VCAM-1 and E-selectin. Cytokine-induced expression of these genes is dependent on NF-κB activation, based on promoter deletion studies, which demonstrated that NF-κB sites are necessary but not sufficient for transcription (93-96). LPS treatment of mice induced a dose-dependent increase in expression of both VCAM-1 and E-selectin in the HP region. In the LP region, low expression levels were found even at the 100 μg dose of LPS. Overall these results suggest a strong correlation between nuclear translocation of p65 and expression of VCAM-1 and E-selectin. E-selectin expression was not detected in either HP or LP regions of control mice, in contrast to VCAM-1. This may reflect differences in sensitivities of these genes to NF-κB activation. Expression of PECAM-1 and ICAM-2 did not change in response to LPS treatment and was comparable in the HP and LP regions. Both genes are known to be expressed constitutively by endothelial cells. *In vivo*, PECAM-1 expression on endothelium is not upregulated by inflammatory cytokines (83), although its

promoter contains 2 putative NF-κB binding sites (97). Similarly, ICAM-2 expression is not upregulated in cultured endothelium by cytokines (84).

The series of experiments in this study indicated that the NF-κB signal transduction pathway in endothelium of HP regions was primed to respond to systemic activation stimuli, including ingestion of an atherogenic diet. The HP and LP regions that we studied likely represent two extremes of a spectrum. Our preliminary observations of the mouse descending thoracic aorta support this concept. In parallel to NF-κB, it is likely that other signal transduction pathways or transcription factors are upregulated by vascular cells in a regional fashion. For example, Egr-1 is a transcription factor that can be induced by acute stimuli, including shear stress, and is upregulated in the intima of atherosclerotic lesions (98). Regional differences in only a few signaling pathways or transcription factors may result in dramatically different biological responses to systemic activation stimuli, because each pathway and transcription factors can regulate the expression of multiple genes.

SUMMARY

In summary, we have developed a model which permits *en face* analysis of gene expression in high probability (HP) and low probability (LP) regions for atherosclerotic lesion development, corresponding to the greater and lesser curvature of the ascending aorta and aortic arch respectively. Since the two regions were mapped on a single piece of tissue , this allowed for meaningful comparative quantitation of components in HP vs LP regions.

Silver nitrate staining showed HP regions cells were polygonal in shape, more densely packed and randomly oriented, in contrast to LP region cells which were elongated in shape and aligned in the direction of blood flow. This suggested regional hemodynamic differences in HP and LP regions.

Despite that fact that expression levels of key endothelial cell NF-κB components (p65, IκBα and IκBβ) were dramatically elevated in HP regions of control mice, activation of NF-κB was found in only a minority of endothelial cells. This suggested that the NF-κB signal transduction pathway was "pumped up" in HP regions and that these regions were primed to respond upon encountering appropriate activation stimuli.

Treatment with bacterial endotoxin or feeding a cholesterol rich diet, selectively induced p65 nuclear translocation in HP regions whereas the LP regions remained largely quiescent.

NF-κB target genes VCAM-1 and E-selectin showed increased expression in HP regions following LPS stimulation whereas control genes ICAM-2 and PECAM-1 showed comparable expression in HP and LP regions.

These data suggest a mechanism for how localized gene expression and atherosclerotic lesion formation can occur in response to systemic stimuli. Although hemodynamics is likely involved, its precise role remains to be determined.

FUTURE DIRECTIONS

Perhaps, the most interesting finding in this study is the dramatically elevated levels of NF-κB components in HP as compared to LP regions in control mice. The subsequent results including increased NF-κB activation in HP regions of control mice and a further increase upon superimposition of atherogenic stimuli are likely to be governed by the initial differences in expression levels or different set points. A promising next step might be to look at regulation of p65 expression, since little data is available, to date.

This study suggests a role for hemodynamics in upregulating the NF-κB signal transduction pathway in HP regions. Mapping HP and LP regions in an area of the aorta that could later be surgically manipulated (eg. ligation of renal artery) would permit studies that would solidify and reveal details about the precise role of hemodynamics.

Although this study reveals a strong correlation between NF-κB activation and induction of target gene expression in HP regions, inhibition studies are required to suggest a causal link. As new, specific inhibitors of NF-κB activation become available, these studies will become more feasible.

Finally, this study suggests that NF-κB signal transduction is upregulated in HP regions causing upregulation of pro-atherogenic target genes, contributing to lesion initiation. Alternatively, it is possible that NF-κB signal transduction is downregulated in LP regions or that other signal transduction pathways may be upregulated in LP regions, which dictate the expression of atheroprotective genes. Future studies aimed at comparing expression of atheroprotective genes in HP vs. LP regions and subsequently studying relevant signal transduction cascades will be helpful in creating a more holistic picture.

REFERENCES

1. Breslow, J.L. 1997. Cardiovascular disease burden increases, NIH funding decreases. *Nat Med.* 3:600-601.

2. Fuster, V., R. Ross, and E.J. Topol. 1996. Atherosclerosis and Coronary Artery Disease. Lippincott-Raven, Philadelphia.

3. Ross, R. 1999. Atherosclerosis - an inflammatory disease. *New England Journal of Medicine.* 340:115-126.

4. Gerrity, R.G. 1981. The role of the monocyte in atherogenesis: I. Transition of blood-borne monocytes into foam cells in fatty lesions. *American Journal of Pathology.* 103:181-190.

5. Munro, J.M., and R.S. Cotran. 1988. The pathogenesis of atherosclerosis: atherogenesis and inflammation. *Laboratory Investigation.* 58:249-261.

6. Rosenfeld, M.E., T. Tsukada, A.M. Gown, and R. Ross. 1987. Fatty streak initiation in Watanabe Heritable Hyperlipemic and comparably hypercholesterolemic fat-fed rabbits. *Arteriosclerosis.* 7:9-23.

7. Rosenfeld, M.E., T. Tsukada, A. Chait, E.L. Bierman, A.M. Gown, and R. Ross. 1987. Fatty streak expansion and maturation in Watanabe Heritable Hyperlipemic and comparably hypercholesterolemic fat-fed rabbits. *Arteriosclerosis.* 7:24-34.

8. Gerrity, R.G. 1981. The role of the monocyte in atherogenesis: II. Migration of foam cells from atherosclerotic lesions. *Am J Pathol.* 103:191-200.

9. Gerrity, R.G., H.K. Naito, M. Richardson, and C.J. Schwartz. 1979. Dietary induced atherogenesis in swine. Morphology of the intima in prelesion stages. *Am J Pathol.* 95:775-792.

10. Jerome, W.G., and J.C. Lewis. 1985. Early atherogenesis in White Carneau pigeons. II. Ultrastructural and cytochemical observations. *Am J Pathol.* 119:210-222.

11. Masuda, J., and R. Ross. 1990. Atherogenesis during low level hypercholesterolemia in the nonhuman primate. II. Fatty streak conversion to fibrous plaque. *Arteriosclerosis*. 10:178-187.

12. Masuda, J., and R. Ross. 1990. Atherogenesis during low level hypercholesterolemia in the nonhuman primate. I. Fatty streak formation. *Arteriosclerosis*. 10:164-177.

13. Reddick, R.L., S.H. Zhang, and N. Maeda. 1994. Atherosclerosis in mice lacking apo E. Evaluation of lesional development and progression [published erratum appears in Arterioscler Thromb 1994 May;14(5):839]. *Arterioscler Thromb*. 14:141-147.

14. Nakashima, Y., A.S. Plump, E.W. Raines, J.L. Breslow, and R. Ross. 1994. ApoE-deficient mice develop lesions of all phases of atherosclerosis throughout the arterial tree. *Arteriosclerosis & Thrombosis*. 14:133-140.

15. Steinberg, D., S. Parthasarathy, T.E. Carew, J.C. Khoo, and J.L. Witztum. 1989. Beyond cholesterol. Modifications of low-density lipoprotein that increase its atherogenicity [see comments]. *N Engl J Med*. 320:915-924.

16. Steinberg, D., T.E. Carew, C. Fielding, A.M. Fogelman, R.W. Mahley, A.D. Sniderman, and D.B. Zilversmit. 1989. Lipoproteins and the pathogenesis of atherosclerosis. *Circulation*. 80:719-723.

17. Nievelstein, P.F., A.M. Fogelman, G. Mottino, and J.S. Frank. 1991. Lipid accumulation in rabbit aortic intima 2 hours after bolus infusion of low density lipoprotein. A deep-etch and immunolocalization study of ultrarapidly frozen tissue. *Arterioscler Thromb*. 11:1795-1805.

18. Schwenke, D.C., and T.E. Carew. 1989. Initiation of atherosclerotic lesions in cholesterol-fed rabbits. II. Selective retention of LDL vs. selective increases in LDL permeability in susceptible sites of arteries. *Arteriosclerosis*. 9:908-918.

19. Freeman, M., J. Ashkenas, D.J. Rees, D.M. Kingsley, N.G. Copeland, N.A. Jenkins, and M. Krieger. 1990. An ancient, highly conserved family of cysteine-rich protein

domains revealed by cloning type I and type II murine macrophage scavenger receptors. *Proc Natl Acad Sci U S A.* 87:8810-8814.

20. Pober, J.S., and R.S. Cotran. 1990. Cytokines and endothelial cell biology. *Physiol Rev.* 70:427-451.

21. Etingin, O.R., R.L. Silverstein, H.M. Friedman, and D.P. Hajjar. 1990. Viral activation of the coagulation cascade: molecular interactions at the surface of infected endothelial cells. *Cell.* 61:657-662.

22. Davies, P.F., and S.C. Tripathi. 1993. Mechanical stress mechanisms and the cell. An endothelial paradigm. *Circ Res.* 72:239-245.

23. Parhami, F., Z.T. Fang, A.M. Fogelman, A. Andalibi, M.C. Territo, and J.A. Berliner. 1993. Minimally modified low density lipoprotein-induced inflammatory responses in endothelial cells are mediated by cyclic adenosine monophosphate. *J Clin Invest.* 92:471-478.

24. Berliner, J.A., D.S. Schwartz, M.C. Territo, A. Andalibi, L. Almada, A.J. Lusis, D. Quismorio, Z.P. Fang, and A.M. Fogelman. 1993. Induction of chemotactic cytokines by minimally oxidized LDL. *Adv Exp Med Biol.* 351:13-18.

25. Murphy-Chutorian, D., and E.L. Alderman. 1994. The case that hyperhomocysteinemia is a risk factor for coronary artery disease. *Am J Cardiol.* 73:705-707.

26. Gimbrone, M.A., Jr. 1987. Vascular endothelium: nature's blood-compatible container. *Ann N Y Acad Sci.* 516:5-11.

27. Ross, R. 1993. The pathogenesis of atherosclerosis: a perspective for the 1990s. *Nature.* 362:801-809.

28. Gimbrone, M.A., Jr. 1989. Endothelial dysfunction and atherosclerosis. *J Card Surg.* 4:180-183.

29. Cybulsky, M.I., and M.A. Gimbrone, Jr. 1991. Endothelial expression of a mononuclear leukocyte adhesion molecule during atherogenesis. *Science.* 251:788-791.

30. Olofsson, A.M., K.E. Arfors, L. Ramezani, B.A. Wolitzky, E.C. Butcher, and U.H. von Andrian. 1994. E-selectin mediates leukocyte rolling in interleukin-1-treated rabbit mesentery venules. *Blood.* 84:2749-2758.

31. Alon, R., P.D. Kassner, M.W. Carr, E.B. Finger, M.E. Hemler, and T.A. Springer. 1995. The integrin VLA-4 supports tethering and rolling in flow on VCAM-1. *J Cell Biol.* 128:1243-1253.

32. Cushing, S.D., J.A. Berliner, A.J. Valente, M.C. Territo, M. Navab, F. Parhami, R. Gerrity, C.J. Schwartz, and A.M. Fogelman. 1990. Minimally modified low density lipoprotein induces monocyte chemotactic protein 1 in human endothelial cells and smooth muscle cells. *Proc Natl Acad Sci U S A.* 87:5134-5138.

33. Berliner, J.A., M. Territo, L. Almada, A. Carter, E. Shafonsky, and A.M. Fogelman. 1986. Monocyte chemotactic factor produced by large vessel endothelial cells in vitro. *Arteriosclerosis.* 6:254-258.

34. Rosenfeld, M.E., W. Palinski, S. Yla-Herttuala, and T.E. Carew. 1990. Macrophages, endothelial cells, and lipoprotein oxidation in the pathogenesis of atherosclerosis. *Toxicol Pathol.* 18:560-571.

35. Gimbrone, M.A., Jr., N. Resnick, T. Nagel, L.M. Khachigian, T. Collins, and J.N. Topper. 1997. Hemodynamics, endothelial gene expression, and atherogenesis. *Ann N Y Acad Sci.* 811:1-10; discussion 10-11.

36. Texon, M. 1977. The hemodynamic basis of atherosclerosis. *Adv Exp Med Biol.* 82:180-181.

37. Gyurko, G., and M. Szabo. 1969. Experimental investigations of the role of hemodynamic factors in formation of intimal changes. *Surgery.* 66:871-874.

38. Imparato, A.M., J.W. Lord, Jr., M. Texon, and M. Helpern. 1961. Experimental atherosclerosis produced by alteration of blood vessel configuration. *Surgical Forum.* 12:245-247.

39. Giddens, D.P., C.K. Zarins, and S. Glagov. 1993. The role of fluid mechanics in the localization and detection of atherosclerosis. *J Biomech Eng*. 115:588-594.

40. el-Masry, O.A., I.A. Feuerstein, and G.F. Round. 1978. Experimental evaluation of streamline patterns and separated flows in a series of branching vessels with implications for atherosclerosis and thrombosis. *Circ Res*. 43:608-618.

41. Ku, D.N., and C. Zhu. 1993. The mechanical environment of the artery. *In* Hemodynamic forces and vascular cell biology. B.E. Sumpio, editor. R.G. Landes Company, Austin. 1-23.

42. Perktold, K., M. Resch, and H. Florian. 1991. Pulsatile non-Newtonian flow characteristics in a three-dimensional human carotid bifurcation model. *J Biomech Eng*. 113:464-475.

43. Perktold, K., M. Resch, and R.O. Peter. 1991. Three-dimensional numerical analysis of pulsatile flow and wall shear stress in the carotid artery bifurcation. *J Biomech*. 24:409-420.

44. Truskey, G.A., R.A. Herrmann, J. Kait, and K.M. Barber. 1999. Focal increases in vascular cell adhesion molecule-1 and intimal macrophages at atherosclerosis-susceptible sites in the rabbit aorta after short-term cholesterol feeding. *Arterioscler Thromb Vasc Biol*. 19:393-401.

45. Nakashima, Y., E.W. Raines, A.S. Plump, J.L. Breslow, and R. Ross. 1998. Upregulation of VCAM-1 and ICAM-1 at atherosclerosis-prone sites on the endothelium in the ApoE-deficient mouse. *Arteriosclerosis, Thrombosis & Vascular Biology*. 18:842-851.

46. Back, M.R., T.E. Carew, and G.W. Schmid-Schoenbein. 1995. Deposition pattern of monocytes and fatty streak development in hypercholesterolemic rabbits. *Atherosclerosis*. 116:103-115.

47. Levesque, M.J., and R.M. Nerem. 1985. The elongation and orientation of cultured endothelial cells in response to shear stress. *Journal of Biomechanical Engineering*. 107:341-347.

48. Levesque, M.J., D. Liepsch, S. Moravec, and R.M. Nerem. 1986. Correlation of endothelial cell shape and wall shear stress in a stenosed dog aorta. *Arteriosclerosis*. 6:220-229.

49. Reidy, M.A., and B.L. Langille. 1980. The effect of local blood flow patterns on endothelial cell morphology. *Experimental & Molecular Pathology*. 32:276-289.

50. Langille, B.L., and S.L. Adamson. 1981. Relationship between blood flow direction and endothelial cell orientation at arterial branch sites in rabbits and mice. *Circulation Research*. 48:481-488.

51. Langille, B.L., and F. O'Donnell. 1986. Reductions in arterial diameter produced by chronic decreases in blood flow are endothelium-dependent. *Science*. 231:405-407.

52. Langille, B.L., M.A. Reidy, and R.L. Kline. 1986. Injury and repair of endothelium at sites of flow disturbances near abdominal aortic coarctations in rabbits. *Arteriosclerosis*. 6:146-154.

53. Wechezak, A.R., R.F. Viggers, and L.R. Sauvage. 1985. Fibronectin and F-actin redistribution in cultured endothelial cells exposed to shear stress. *Lab Invest*. 53:639-647.

54. Dewey, C.F., Jr., S.R. Bussolari, M.A. Gimbrone, Jr., and P.F. Davies. 1981. The dynamic response of vascular endothelial cells to fluid shear stress. *J Biomech Eng*. 103:177-185.

55. Malek, A.M., G.H. Gibbons, V.J. Dzau, and S. Izumo. 1993. Fluid shear stress differentially modulates expression of genes encoding basic fibroblast growth factor and platelet-derived growth factor B chain in vascular endothelium. *J Clin Invest*. 92:2013-2021.

56. Karin, M. 1999. The beginning of the end: IkB kinase (IKK) and NF-kB activation. *Journal of Biological Chemistry*. 274:27339-27342.

57. Ghosh, S., M.J. May, and E.B. Kopp. 1998. NF-kappa B and Rel proteins: evolutionarily conserved mediators of immune responses. *Annual Review of Immunology*. 16:225-260.

58. Read, M.A., M.Z. Whitley, A.J. Williams, and T. Collins. 1994. NF-kappa B and I kappa B alpha: an inducible regulatory system in endothelial activation. *Journal of Experimental Medicine*. 179:503-512.

59. Sheppard, K.A., D.W. Rose, Z.K. Haque, R. Kurokawa, E. McInerney, S. Westin, D. Thanos, M.G. Rosenfeld, C.K. Glass, and T. Collins. 1999. Transcriptional activation by NF-kappaB requires multiple coactivators. *Molecular & Cellular Biology*. 19:6367-6378.

60. de Martin, R., B. Vanhove, Q. Cheng, E. Hofer, V. Csizmadia, H. Winkler, and F.H. Bach. 1993. Cytokine-inducible expression in endothelial cells of an I kappa B alpha-like gene is regulated by NF kappa B. *EMBO Journal*. 12:2773-2779.

61. Brown, K., S. Park, T. Kanno, G. Franzoso, and U. Siebenlist. 1993. Mutual regulation of the transcriptional activator NF-kappa B and its inhibitor, I kappa B-alpha. *Proceedings of the National Academy of Sciences of the United States of America*. 90:2532-2536.

62. Scott, M.L., T. Fujita, H.C. Liou, G.P. Nolan, and D. Baltimore. 1993. The p65 subunit of NF-kappa B regulates I kappa B by two distinct mechanisms. *Genes & Development*. 7:1266-1276.

63. Sun, S.C., P.A. Ganchi, D.W. Ballard, and W.C. Greene. 1993. NF-kappa B controls expression of inhibitor I kappa B alpha: evidence for an inducible autoregulatory pathway. *Science*. 259:1912-1915.

64. Arenzana-Seisdedos, F., J. Thompson, M.S. Rodriguez, F. Bachelerie, D. Thomas, and R.T. Hay. 1995. Inducible nuclear expression of newly synthesized I kappa B alpha negatively regulates DNA-binding and transcriptional activities of NF-kappa B. *Molecular & Cellular Biology*. 15:2689-2696.

65. Arenzana-Seisdedos, F., P. Turpin, M. Rodriguez, D. Thomas, R.T. Hay, J.L. Virelizier, and C. Dargemont. 1997. Nuclear localization of I kappa B alpha promotes active transport of NF-kappa B from the nucleus to the cytoplasm. *Journal of Cell Science*. 110:369-378.

66. Brand, K., T. Eisele, U. Kreusel, M. Page, S. Page, M. Haas, A. Gerling, C. Kaltschmidt, F.J. Neumann, N. Mackman, P.A. Baeurele, A.K. Walli, and D. Neumeier. 1997. Dysregulation of monocytic nuclear factor-kappa B by oxidized low- density lipoprotein. *Arterioscler Thromb Vasc Biol.* 17:1901-1909.

67. Cominacini, L., U. Garbin, A.F. Pasini, A. Davoli, M. Campagnola, A.M. Pastorino, G. Gaviraghi, and V. Lo Cascio. 1998. Oxidized low-density lipoprotein increases the production of intracellular reactive oxygen species in endothelial cells: inhibitory effect of lacidipine. *J Hypertens.* 16:1913-1919.

68. Carluccio, M.A., M. Massaro, C. Bonfrate, L. Siculella, M. Maffia, G. Nicolardi, A. Distante, C. Storelli, and R. De Caterina. 1999. Oleic acid inhibits endothelial activation : A direct vascular antiatherogenic mechanism of a nutritional component in the mediterranean diet. *Arterioscler Thromb Vasc Biol.* 19:220-228.

69. Krull, M., A.C. Klucken, F.N. Wuppermann, O. Fuhrmann, C. Magerl, J. Seybold, S. Hippenstiel, J.H. Hegemann, C.A. Jantos, and N. Suttorp. 1999. Signal transduction pathways activated in endothelial cells following infection with Chlamydia pneumoniae. *J Immunol.* 162:4834-4841.

70. Collins, T., M.A. Read, A.S. Neish, M.Z. Whitley, D. Thanos, and T. Maniatis. 1995. Transcriptional regulation of endothelial cell adhesion molecules: NF-kappa B and cytokine-inducible enhancers. *FASEB Journal.* 9:899-909.

71. Murase, T., N. Kume, T. Hase, Y. Shibuya, Y. Nishizawa, I. Tokimitsu, and T. Kita. 1999. Gallates inhibit cytokine-induced nuclear translocation of NF-kappaB and expression of leukocyte adhesion molecules in vascular endothelial cells. *Arterioscler Thromb Vasc Biol.* 19:1412-1420.

72. Hernandez-Presa, M., C. Bustos, M. Ortego, J. Tunon, G. Renedo, M. Ruiz-Ortega, and J. Egido. 1997. Angiotensin-converting enzyme inhibition prevents arterial nuclear factor-kappa B activation, monocyte chemoattractant protein-1 expression, and macrophage infiltration in a rabbit model of early accelerated atherosclerosis. *Circulation.* 95:1532-1541.

73. Gawaz, M., F.J. Neumann, T. Dickfeld, W. Koch, K.L. Laugwitz, H. Adelsberger, K. Langenbrink, S. Page, D. Neumeier, A. Schomig, and K. Brand. 1998. Activated platelets induce monocyte chemotactic protein-1 secretion and surface expression of intercellular adhesion molecule-1 on endothelial cells [see comments]. *Circulation.* 98:1164-1171.

74. Hernandez-Presa, M.A., C. Bustos, M. Ortego, J. Tunon, L. Ortega, and J. Egido. 1998. ACE inhibitor quinapril reduces the arterial expression of NF-kappaB-dependent proinflammatory factors but not of collagen I in a rabbit model of atherosclerosis. *Am J Pathol.* 153:1825-1837.

75. Brand, K., S. Page, G. Rogler, A. Bartsch, R. Brandl, R. Knuechel, M. Page, C. Kaltschmidt, P.A. Baeuerle, and D. Neumeier. 1996. Activated transcription factor nuclear factor-kappa B is present in the atherosclerotic lesion. *J Clin Invest.* 97:1715-1722.

76. Tsao, P.S., R. Buitrago, J.R. Chan, and J.P. Cooke. 1996. Fluid flow inhibits endothelial adhesiveness. Nitric oxide and transcriptional regulation of VCAM-1. *Circulation.* 94:1682-1689.

77. Bao, X., C. Lu, and J.A. Frangos. 1999. Temporal gradient in shear but not steady shear stress induces PDGF-A and MCP-1 expression in endothelial cells: role of NO, NF kappa B, and egr-1. *Arteriosclerosis, Thrombosis & Vascular Biology.* 19:996-1003.

78. Mohan, S., N. Mohan, and E.A. Sprague. 1997. Differential activation of NF-kappa B in human aortic endothelial cells conditioned to specific flow environments. *American Journal of Physiology.* 273:C572-578.

79. Mohan, S., N. Mohan, A.J. Valente, and E.A. Sprague. 1999. Regulation of low shear flow-induced HAEC VCAM-1 expression and monocyte adhesion. *American Journal of Physiology*. 276:C1100-1107.

80. Lichtman, A.H., S.K. Clinton, K. Iiyama, P.W. Connelly, P. Libby, and M.I. Cybulsky. 1999. Hyperlipidemia and atherosclerotic lesion development in LDL receptor-deficient mice fed defined semipurified diets with and without cholate. *Arteriosclerosis, Thrombosis & Vascular Biology*. 19:1938-1944.

81. Flaherty, J.T., J.E. Pierce, V.J. Ferrans, D.J. Patel, W.K. Tucker, and D.L. Fry. 1972. Endothelial nuclear patterns in the canine arterial tree with particular reference to hemodynamic events. *Circulation Research*. 30:23-33.

82. Remuzzi, A., C.F. Dewey, Jr., P.F. Davies, and M.A. Gimbrone, Jr. 1984. Orientation of endothelial cells in shear fields in vitro. *Biorheology*. 21:617-630.

83. Henninger, D.D., J. Panes, M. Eppihimer, J. Russell, M. Gerritsen, D.C. Anderson, and D.N. Granger. 1997. Cytokine-induced VCAM-1 and ICAM-1 expression in different organs of the mouse. *Journal of Immunology*. 158:1825-1832.

84. Xu, H., J.K. Bickford, E. Luther, C. Carpenito, F. Takei, and T.A. Springer. 1996. Characterization of murine intercellular adhesion molecule-2. *Journal of Immunology*. 156:4909-4914.

85. Nagel, T., N. Resnick, C.F. Dewey, Jr., and M.A. Gimbrone, Jr. 1999. Vascular endothelial cells respond to spatial gradients in fluid shear stress by enhanced activation of transcription factors. *Arteriosclerosis, Thrombosis & Vascular Biology*. 19:1825-1834.

86. DePaola, N., M.A. Gimbrone, Jr., P.F. Davies, and C.F. Dewey, Jr. 1992. Vascular endothelium responds to fluid shear stress gradients. *Arteriosclerosis & Thrombosis*. 12:1254-1257.

87. Takahashi, M., T. Ishida, O. Traub, M.A. Corson, and B.C. Berk. 1997. Mechanotransduction in endothelial cells: temporal signaling events in response to shear stress. *Journal of Vascular Research*. 34:212-219.

88. Traub, O., and B.C. Berk. 1998. Laminar shear stress: mechanisms by which endothelial cells transduce an atheroprotective force. *Arteriosclerosis, Thrombosis & Vascular Biology*. 18:677-685.

89. Topper, J.N., J. Cai, D. Falb, and M.A. Gimbrone, Jr. 1996. Identification of vascular endothelial genes differentially responsive to fluid mechanical stimuli: cyclooxygenase-2, manganese superoxide dismutase, and endothelial cell nitric oxide synthase are selectively up-regulated by steady laminar shear stress. *Proceedings of the National Academy of Sciences of the United States of America*. 93:10417-10422.

90. Schwenke, D.C. 1995. Selective increase in cholesterol at atherosclerosis-susceptible aortic sites after short-term cholesterol feeding. *Arteriosclerosis, Thrombosis & Vascular Biology*. 15:1928-1937.

91. Schussheim, A.E., and V. Fuster. 1999. Antibiotics for myocardial infarction? A possible role of infection in atherogenesis and acute coronary syndromes. *Drugs*. 57:283-291.

92. Calara, F., P. Dimayuga, A. Niemann, J. Thyberg, U. Diczfalusy, J.L. Witztum, W. Palinski, P.K. Shah, B. Cercek, J. Nilsson, and J. Regnstrom. 1998. An animal model to study local oxidation of LDL and its biological effects in the arterial wall. *Arteriosclerosis, Thrombosis & Vascular Biology*. 18:884-893.

93. Whelan, J., P. Ghersa, R. Hooft van Huijsduijnen, J. Gray, G. Chandra, F. Talabot, and J.F. DeLamarter. 1991. An NF kappa B-like factor is essential but not sufficient for cytokine induction of endothelial leukocyte adhesion molecule 1 (ELAM-1) gene transcription. *Nucleic Acids Research*. 19:2645-2653.

94. Whitley, M.Z., D. Thanos, M.A. Read, T. Maniatis, and T. Collins. 1994. A striking similarity in the organization of the E-selectin and beta interferon gene promoters. *Molecular & Cellular Biology*. 14:6464-6475.

95. Iademarco, M.F., J.J. McQuillan, G.D. Rosen, and D.C. Dean. 1992. Characterization of the promoter for vascular cell adhesion molecule-1 (VCAM-1). *Journal of Biological Chemistry*. 267:16323-16329.

96. Neish, A.S., A.J. Williams, H.J. Palmer, M.Z. Whitley, and T. Collins. 1992. Functional analysis of the human vascular cell adhesion molecule 1 promoter. *Journal of Experimental Medicine*. 176:1583-1593.

97. Gumina, R.J., N.E. Kirschbaum, K. Piotrowski, and P.J. Newman. 1997. Characterization of the human platelet/endothelial cell adhesion molecule-1 promoter: identification of a GATA-2 binding element required for optimal transcriptional activity. *Blood*. 89:1260-1269.

98. McCaffrey, T.A., C. Fu, B. Du, S. Eksinar, K.C. Kent, H. Bush, Jr., K. Kreiger, T. Rosengart, M.I. Cybulsky, E.S. Silverman, and T. Collins. 2000. High-level expression of Egr-1 and Egr-1-inducible genes in mouse and human atherosclerosis. *Journal of Clinical Investigation*. 105:653-662.